E949 Technical Note K-074

Analysis of the 2/3 E949 pnn2 data

Joss Ives, Benji Lewis, Zhe Wang, David E. Jaffe

March 4, 2008

Abstract

Contents

List of Figures

List of Tables

Background Component	Entire "Loose"	Cleanest cell "Tight"
$K_{\pi 2}$TT scatter	$0.575 \pm 0.184^{+0.063}_{-0.201}$	$0.115 \pm 0.058^{+0.039}_{-0.022}$
$K_{\pi 2}$RS scatter	-0.0070 ± 0.0042	-0.0031 ± 0.0018
$K_{\pi 2\gamma}$	$0.0500 \pm 0.0084 \pm 0.0030$	$0.0182 \pm 0.0047 \pm 0.0011$
K_{e4}	$0.176 \pm 0.102^{+0.233}_{-0.124}$	$0.034 \pm 0.034^{+0.142}_{-0.026}$
CEX	$0.092 \pm 0.053^{+0.070}_{-0.018}$	$0.0046 \pm 0.0046^{+0.0046}_{-0.0015}$
Muon	0.0281 ± 0.0281	0.00374 ± 0.00374
Two-beam	0.0438 ± 0.0200	0.00317 ± 0.00317
One-beam	0.00157 ± 0.00157	0.00035 ± 0.00035
Total Background	$0.966 \pm 0.220^{+0.309}_{-0.246}$	$0.179 \pm 0.068^{+0.152}_{-0.035}$
Total Acceptance	$(1.841 \pm 0.065^{+0.194}_{-0.194}) \times 10^{-3}$	$(0.600 \pm 0.176^{+0.063}_{-0.064}) \times 10^{-3}$
Single-event sensitivity	$(0.432 \pm 0.015^{+0.046}_{-0.046}) \times 10^{-9}$	$(1.325 \pm 0.389^{+0.141}_{-0.143}) \times 10^{-9}$

Table 1: The estimated backgrounds for the entire signal region, referred to as "loose" elsewhere in the text, and the cleanest cell, referred to as "tight", to be used in the analysis. The first error is the statistical uncertainty; the second error (when present) is the estimated systematic uncertainty. The systematic uncertainties for the K_{e4} and CEX backgrounds are assumed to be fully correlated. The cleanest cell corresponds to the tight settings of the KIN, TD, PV and DELCO cuts. The background due to $K_{\pi 2}$RS scatters is assumed to be negligible and not included in the totals. The bottom rows contains the total acceptance and single event sensitivity of the two regions. The acceptance given in the table does not include the additional factors of $f_S = 0.7740 \pm 0.0011$ and $\epsilon_{T\bullet 2} = 0.9505 \pm 0.0012 \pm 0.0143$.

1 Executive Summary

Expected backgrounds from the 1/3 and 2/3 analyses are given in Table 1 as well as the single event sensitivity and total acceptance. A number of small changes to the analysis have occurred since Technical Note K-073 [1] that described all the changes to the analysis with respect to the prior pnn2 analysis and the E949 pnn1 analysis. None of these changes had a profound effect on the conclusions from the 1/3 note.

This note is organized as follows. Section 2 summarizes the changes with respect to the 1/3 analysis note [1]. The $K_{\pi 2}$-scatter, $K_{\pi 2\gamma}$, beam, muon, charge exchange (CEX) and K_{e4} background estimates are given in Sections 3, 4, 5, 6, 7 and 8, respectively. Studies to ascertain the effect of contamination of background samples is presented in 9. Section 10 describes the acceptance measuremnts and Section 11 contains the description of the kaon exposure. The investigation of flaws and loopholes with a single-cut-failure study is described in Section 12. The sensitivity of the analysis is evaluated in Section 13.

2 Summary of changes with respect to the 1/3 analysis note

Several changes to the analysis were made subsequent to the 1/3 analysis note [1]. None of the changes had a significant effect on the background or acceptance estimates. The changes are

1. Fix to the CCDBADTIM cut. This cut requires consistency between the fitted first pulse and the global kaon time. Originally this cut was only placed on the first fitted pulse for fibers with double-pulse fits only. While searching by visual scan for evidence of K_{e4} contamination in the $K_{\pi 2}$ target-scatter 1/3 normalization branch, an event was observed that showed that the same requirements should be placed on the fitted pulse of single-pulse fits to avoid a possible loophole. Described fully in Section 2.1.

2. (Benji) The evaluation of the single beam background revealed that an unused cut, E787_CCDPUL, had an unintended effect on the CCDPUL cut. Described fully in Section 2.2.

3. (Benji) A coding error affected the muon normalization branch. Described fully in Section 2.3.

4. (Benji) Deprecated cuts related to target dE/dx were inadvertently applied in the beam normalization branch. Described fully in Section 2.4.

5. The multiplexing of low-gain CCD fibers was not correctly taken into account. Described fully in Sections 2.5 (Benji) and 2.6 (Joss).

2.1 CCDBADTIM fix

The CCDBADTIM was originally designed to remove events having double-pulse fit time values consistent with incorrect fitter solutions. During a visual scan of tg-scatter normalization events, an event like that found in Figure 1 was observed. The double-pulse fits were never performed on either the logain or the higain due to the single-fit probabilities for both gain channels being above 0.25. For both gain channels, the single-pulse time is consistent with *tpi* (global pion time) and not *tk* (global kaon time). Due to most of the energy being in the second pulse, the fitter found a reasonable solution for the single-pulse fit by fitting the second pulse. Observation of this type of event brought to our attention that the same conditions checked by CCDBADTIM on the first-pulse of the double-pulse fit also need to be applied to the single-pulse.

For each fiber, each of the two gain channels are checked to see if they have a single-fit probability above 0.25 and that the energy from ADC is above 1.25 MeV. If so, the same time conditions are checked for the single-pulse fit as are checked for the first-pulse on the double-pulse fit. If either of these conditions are met, that gain channel is flagged for possible rejection by CCDBADTIM:

- The single-pulse time is less than -9.98 This is the minimum value stored in the ntuple for the first-pulse times from the double-pulse fits;
- The single-pulse time (t_0) is not consistent with the global kaon time tk. The failing conditions are $t_0 - tk < -6$ or $t_0 - tk > 7$. Figure 2 shows that these conditions are suitable for times of both the single-pulse fit and the first pulse of the double-pulse fit.

A fiber having a gain channel that has been flagged for possible rejection by CCDBADTIM will cause the event to fail CCDBADTIM if

- Both gain channels have been flagged for possible rejection by CCDBADTIM;
- One gain channel has been flagged for possible rejection by and CCDBADTIM and the other gain channel has a double-pulse fit probability of zero;
- One gain channel has been flagged for possible rejection by and CCDBADTIM and data from the other gain channel is missing;

In addition to these new conditions on the single-pulse time, the previous conditions on the double-pules times are also checked.

2.2 E787_CCDPUL story

The routine `ccdpul_787.function` (the final version of CCDPUL used in E787) had a routines and common blocks with the same name as `ccdpul.function`. Although `ccdpul_787.function` was no longer an "active" cut, the cut was available in Benji's scripts and functions for comparisons purposes. The solution of replacing the cut function with a null cut was implemented. This would remove any other possible conflicts currently unknown.

2.3 Muon background story

To require that only the loose version of TDCUT was inverted (to prevent looking into the box) a direct call to $TDCUT_{loose}$ was performed in Benji's muon-background function. However, during this special implementation the array was not initialized and so some events would be removed due to stale information in the array. The end result did not change. Also, note that this error was not an issue during optimization of the TDCUTs. The error only appeared after the measurements of the tight regions began.

2.4 Beam background story

During E949-PNN2 beam background studies prior to the 2/3 note, the beam background cuts applied RTGHI, ETGHI, TGDEDX1, TGDEDX2 which were part of E949-PNN1's TGDEDX composite cut. TGDEDX cut differs for PNN2 analysis since the kinematic region is much larger than the PNN1 box. Since PNN2 analysis starting point was PNN1's cuts the initial analysis utilized what is now called `tgdedx_pnn1.function`. When the

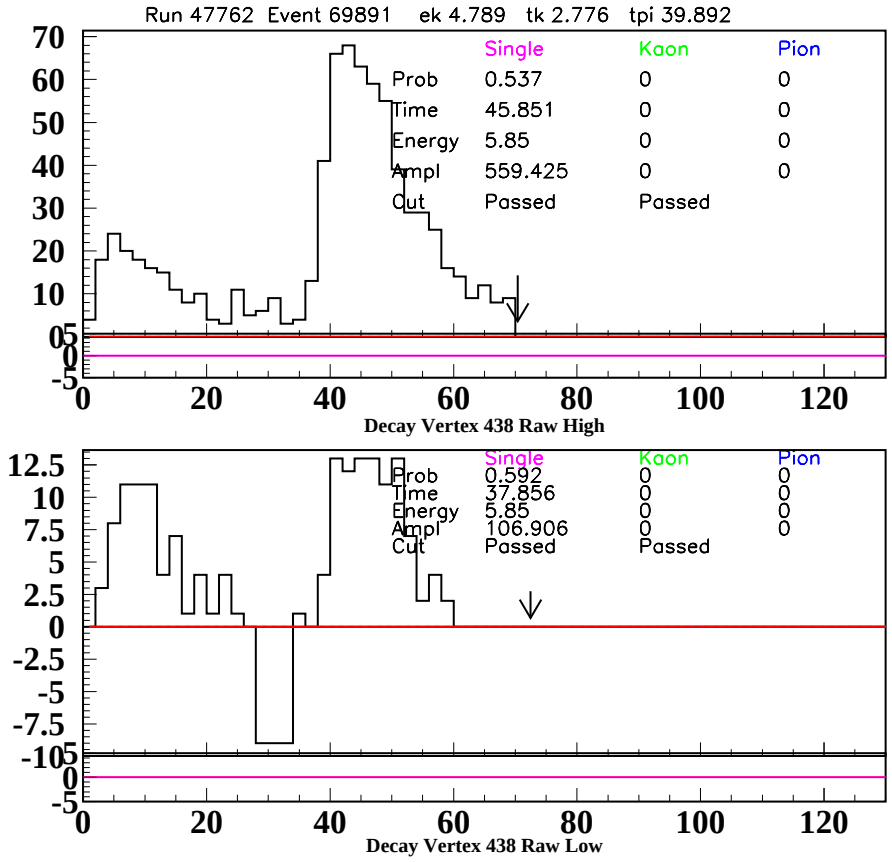

Figure 1: The type of event that motivated the CCDBADTIM fix.

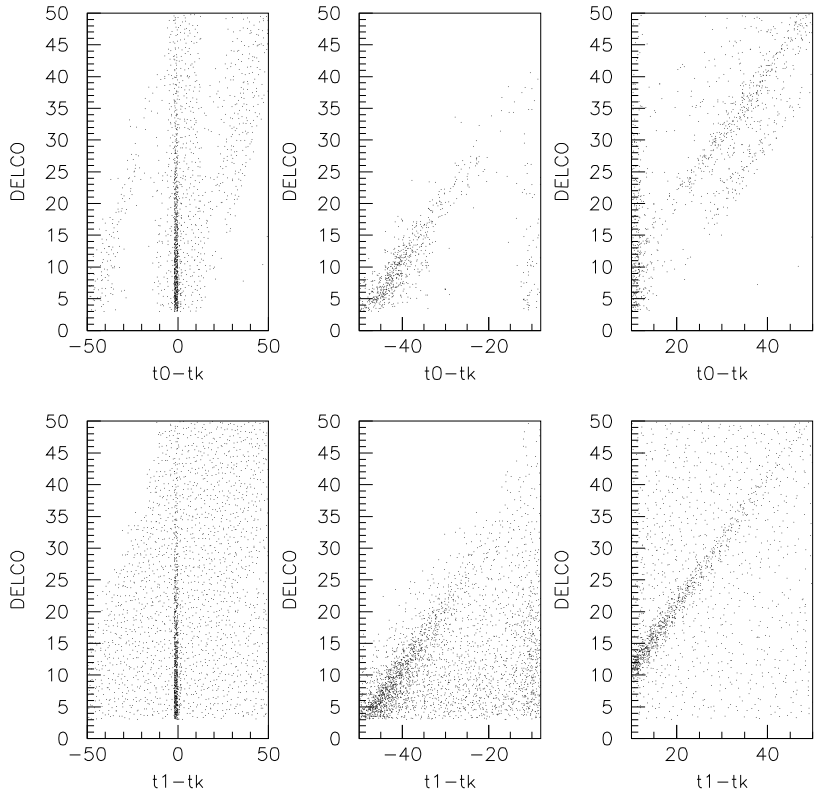

Figure 2: The plots show DELCO vs. the difference between the fitted single-pulse (t0, upper plots) or the first pulse of the double-pulse fit (t1, lower plots) and the global kaon time (tk). DELCO is the difference between the global pion and kaon times (tpi-tk). The central and right-most plots show narrowed x-axis time regions as compared to the left-most plots to emphasize some of the finer structure. The central band around a time of zero in the left-most plots represents good fits. In the upper-right plot, there are two distinct bands. The upper band is DELCO = t0-tk and comes from second (pion) pulses being fit as kaons. The lower band is a result of the 10 ns window around tpi used when fitting.

correct version of TGDEDX was implemented the cuts were not removed from the beam background branches. This oversight had little to no effect on the measured beam background values.

2.5 CCD multiplexing story part 1

The routine `addmux.function` which is employed by the target-CCD routines and is used to correctly accounted for multiplexed energy in the low-gain CCD fibers. `addmux.function` did not correctly consider the time of Photon-Veto hits in the TG (*tpvtg(i)*. *tpvtg* hits were stored relative to *tpi* and other hits within the TG were stored relative to beam strobe. Corrective action was taken as follows:

```
Time = TPVTG(i)
```

became

```
Time = TPVTG(i) + tpi
```

This fixed the specific error which existed during E787-PNN2 analysis.

2.6 CCD multiplexing story part 2

A 1-cut failure (1/3 sample) revealed a mistake in the way low-gain CCD info was being de-multiplexed. Previously the ADC energy for all fibers multiplexed with a given fiber that were within 5ns of *tpi* were summed and subtracted from the fitted 2nd pulse energy. The multiplexed energy was then subtracted from the second pulse. This resulted in total energies between the first and second pulses that were less than the ADC energy of the fiber, which is a mistake since the ADC knows nothing of the multiplexing done with the low-gain CCDs. The algorithm was modified so that energy at both tk and tpi is correctly taken into account when assigning the energy of the 1st and 2d fitted pulse. Modifications were made to `ccdpul.function` and the demultiplexing function `addmux.function`. Additionally, the calls to `addmux.function` from the CCDBADTIM and CCDBADFIT cuts were removed as the amplitudes of the pulses are never actually used.

Here's what was done to `addmux.function`:

1. addmux retains the exact same method of determining the multiplexed energy associated with the second pulse, this energy is now considered the pion multiplexed energy;

2. addmux now looks for kaon fibers (5ns window around *tk*) that are multiplexed with the fiber in questions and returns a kaon multiplexed energy (in addition to the pion multiplexed energy);

3. Since some fibers can be assigned as both kaon and pion fibers, the pion multiplexed energy and kaon multiplexed energy are determined independently. It is possible for the same fiber to contribute to both types of multiplexed energies if the fiber is assigned as kaon and pion. The energy used to determine these energies are *ek_tg* and *epi_tg* respectively.

	Before Fix	After Fix
Rejection	(from $\kappa_{\pi 2}$ target-scatter normalization branch)	
	2991/503 =	2991/500 =
	5.946	5.982
Acceptance	(from Beam/Target acceptance measurement using km21)	
	669207/1262093 =	666042/1262093
	0.5302	0.5277
Acceptance × Rejection		
	3.153	3.157

Table 2: Effects of demultiplexing fix on acceptance and rejection

Here's what was done to CCDPUL:

1. The pion and kaon multiplexed energies are added to the adc energy to get a total energy as seen by the ccd;
2. The energy is split between the two pulses according to the ratio of the fitted amplitudes;
3. The pion and kaon multiplexed energies are then subtracted from their respective pulses;
4. If the resulting pulse energy is below 0.001 MeV, it is assigned an energy of 0.001 MeV. If the resulting pulse energy is above the initial ADC energy, it is assigned the initial ADC energy. Note that if a pulse meets one of these conditions, the other pulse will meet the other condition since the total energy between the two pulses will always equal the inital ADC energy in the kaon fiber.

Table 2 shows the resulting changes to the acceptance and rejection of CCDPUL as a result of the fix. This demultiplexing fix resulted in 3 additional events failing CCDPUL in the loose $K_{\pi 2}$ target-scatter normalization branch (see Table 8). These events are shown in Figures 3 4 and 5.

3 $K_{\pi 2}$-Scatter background

3.1 $K^+ \to \pi^+\pi^o$ Target Scatters

The $K_{\pi 2}$ decay, where the π^+ scatters in the target, is the dominant background for the $\pi\nu\overline{\nu}(2)$ analysis [2]. As it has been shown with Monte Carlo simulations [4] , the photon distribution from the π^o decay is more uniform in polar angle for events where the π^+ has scattered in the target, than for unscattered ones. Therefore, the PV rejection for TG scatter events is expected to be different than that for $K_{\pi 2}$ events in the peak. The π^+ kinematics cannot be used in the bifurcation study, since the PV rejection has to be measured inside the $\pi\nu\overline{\nu}(2)$ kinematic box.

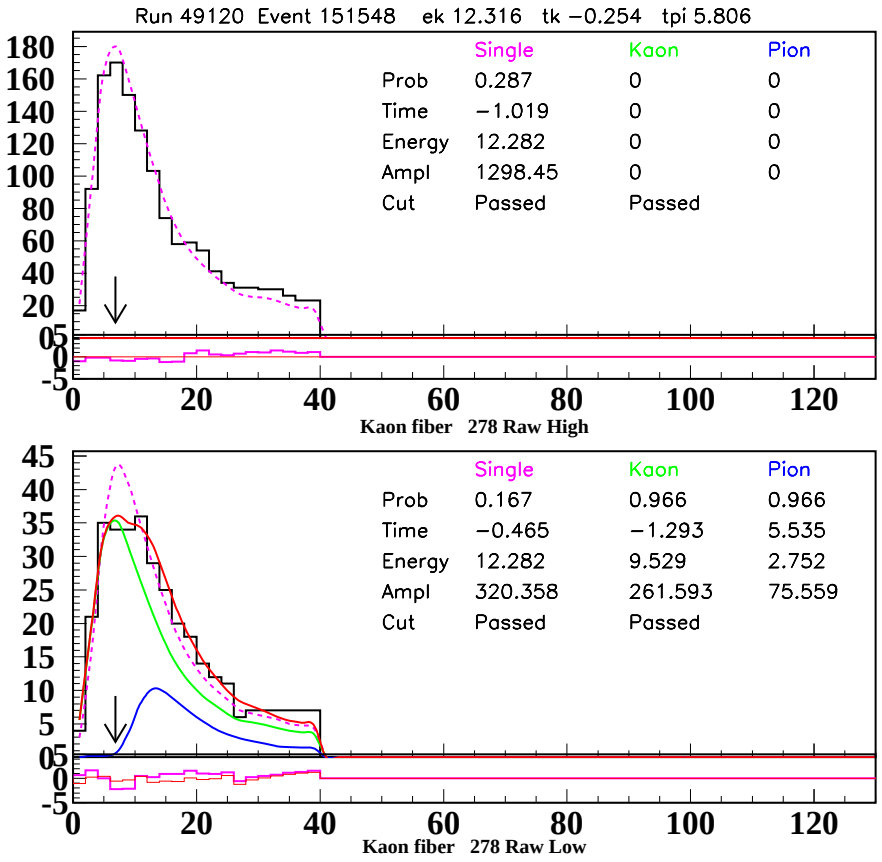

	Before Fix	After Fix
Energy from other multiplexed fibers (MeV)		
E_K(mux)	N/A	0.
E_π(mux)	1.58	1.58
Fitted pulse energy from ADC Energy (MeV)		
Total Energy	12.28	$12.28 + 0.00 + 1.58 = 13.86$
E_K	9.53	10.76
E_π	2.75	3.10
Energy corrected for multiplexed energy (MeV)		
$E_K(corr.)$	9.53	10.76
$E_\pi(corr.)$	$2.75 - 1.58 = 1.17$	$3.10 - 1.58 = 1.52$

Figure 3: Newly Rejected CCDPUL event: run 49120, event 151548. Before demultiplexing fix, the event was passing CCDPUL with 1.17 MeV in the second pulse ($E_\pi(corr.)$) which is below the CCDPUL pion energy threshold of 1.25 MeV. After the demultiplexing fix, the event fails with $E_\pi(corr.) = 1.52$ MeV. This kaon fiber (fiber 278) is multiplexed with a pion fiber with $t = 5.98$ and $E = 1.58$.

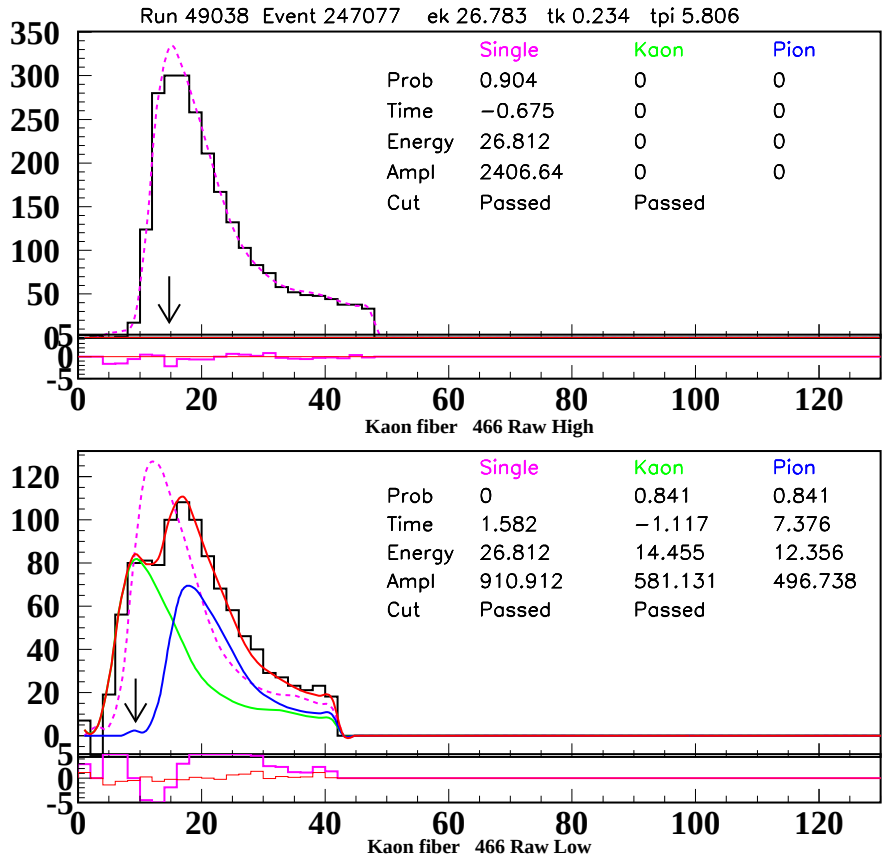

	Before Fix	After Fix
Energy from other multiplexed fibers (MeV)		
E_K(mux)	N/A	0.
E_π(mux)	17.68	17.68
Fitted pulse energy from ADC Energy (MeV)		
Total Energy	26.81	$26.81 + 0.00 + 17.68 = 44.49$
E_K	14.46	24.00
E_π	12.36	20.51
Energy corrected for multiplexed energy (MeV)		
$E_K(corr.)$	14.46	24.00
$E_\pi(corr.)$	$12.35 - 17.68 = -5.33$	$20.51 - 17.68 = 2.83$

Figure 4: Newly Rejected CCDPUL event: run 49038, event 247077. Before demultiplexing fix, the event was passing CCDPUL with 0.001 MeV in the second pulse ($E_\pi(corr.)$) which is below the CCDPUL pion energy threshold of 1.25 MeV. Note that corrected energies below 0.001 MeV are assigned an energy of 0.001 MeV. After the demultiplexing fix, the event fails with $E_\pi(corr.) = 2.83$ MeV. This kaon fiber (fiber 466) is multiplexed with a photon fiber with $t = 1.34$ and $E = 17.68$.

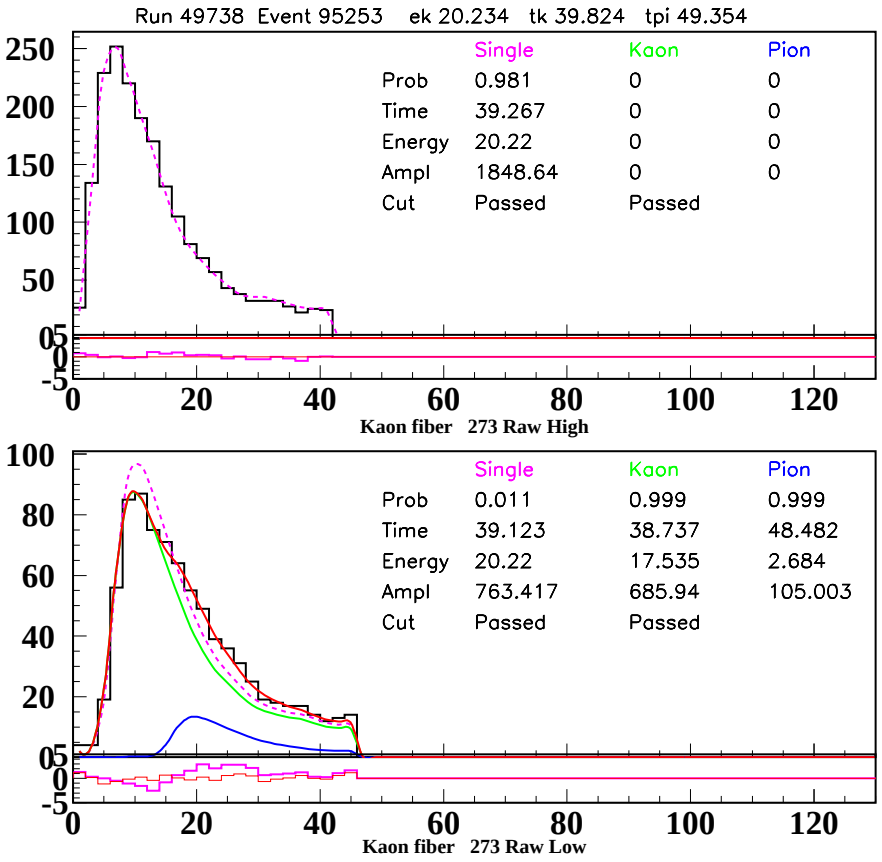

	Before Fix	After Fix
Energy from other multiplexed fibers (MeV)		
E_K(mux)	N/A	0.
E_π(mux)	1.49	1.49
Fitted pulse energy from ADC Energy (MeV)		
Total Energy	20.22	$20.22 + 0.00 + 1.49 = 21.71$
E_K	17.54	18.83
E_π	2.68	2.88
Energy corrected for multiplexed energy (MeV)		
$E_K(corr.)$	17.54	18.83
$E_\pi(corr.)$	$2.68 - 1.49 = 1.19$	$2.88 - 1.49 = 1.39$

Figure 5: Newly Rejected CCDPUL event: run 49738, event 95253.. Before demultiplexing fix, the event was passing CCDPUL with 1.19 MeV in the second pulse ($E_\pi(corr.)$) which is below the CCDPUL pion energy threshold of 1.25 MeV. After the demultiplexing fix, the event fails with $E_\pi(corr.) = 1.39$ MeV. This kaon fiber (fiber 273) is multiplexed with a pion fiber with $t = 48.56$ and $E = 1.49$.

CLASS	TGCUTS
1	All cuts, KP2BOX
2	$\overline{CCDPUL}$, $\overline{EPIONK}$
3	$\overline{CCDPUL}$, $\overline{EPIONK}$, all others
4	CCDPUL, EPIONK, TGZFOOL, EIC, OPSVETO, $\overline{OTHERS}$
5	$\overline{CCDPUL}$, $\overline{EPIONK}$, $\overline{CHI567}$, $\overline{VERRNG}$
6	$\overline{CCDPUL}$, $\overline{EPIONK}$, $\overline{CHI567}$, $\overline{VERRNG}$, all others
7	$\overline{CHI567}$, $\overline{VERRNG}$
8	$\overline{CHI567}$, $\overline{VERRNG}$, all others
9	$\overline{CCDPUL}$, $\overline{EPIONK}$, $\overline{CHI567}$, $\overline{VERRNG}$, KIC, PIGAP, TARGF, TPICS
10	$\overline{B4EKZ}$
11	$\overline{B4EKZ}$, all others
12	$\overline{CCDPUL}$, $\overline{EPIONK}$, $\overline{B4EKZ}$
13	$\overline{CCDPUL}$, $\overline{EPIONK}$, $\overline{B4EKZ}$, all others

Table 3: Definition of the classes of events (2-13) used to measure the PV rejection in the $\pi\nu\overline{\nu}(2)$ kinematic box. Class 1 events have passed all the TG quality cuts, therefore they are required to be in the $K_{\pi 2}$ kinematic box as to not look in the signal region. All Classes that have either CCDPUL applied or CCDPUL inverted have the three associated safety cuts (CCDBADFIT, CCDBADTIM and CCD31FIB) applied. The nomenclature $\overline{CCDPUL}$, $\overline{EPIONK}$ means $\overline{CCDPUL} + \overline{EPIONK}$.

3.1.1 Rejection Branch

The other set of cuts used to suppress this background are the target quality cuts (TGCUT06). These eliminate events with evidence of a scattered pion in the target, either the scatter occurred outside the Kaon fibers (scatters visible in xy, or "xy-scatters") or inside them (events where the π^+ started in the beam direction and then scattered into the detector acceptance, or "z-scatters"). The two categories are not mutually exclusive. By inverting some of these cuts and applying others, samples with varying mixtures of xy- and z-scatters can be created for the rejection branch. These samples will be contaminated to an extent with K_{e4}, $K_{\pi 2\gamma}$ and Charge Exchange background, but the contamination is shown to be small [3]. Thirteen such "classes" were used, described in Table 3, and the PV rejection was measured on them in the $\pi\nu\overline{\nu}(2)$ kinematic box (Table 4) . The PV rejections measured for different classes are consistent with each other within statistical uncertainties.

For the final PV rejection, class 12 was used, because it had adequate statistics and it is expected to be the richest in z-scatters, since the cuts that mainly attack them are inverted: CCDPUL and EPIONK cut events with large pulses in the kaon fibers at trs, and B4EKZ rejects events in which the z position of the decay vertex found by the UTC does not agree with the kaon energy deposit (and thus path length) in the target. Both these signatures are characteristic of a decay pion that started in the beam direction in the kaon fiber, and then scattered into the detector. The difference in PV rejection between different classes with adequate statistics was used as an estimate for

Loose Rejection Branch - Loose PNN2 Box + PV60

CLASS		bef. PV	af. PV	PV Rejection	Background
2	1/3	24466	9	2718.4±906.0	0.552±0.186
	2/3	49183	22	2235.6±476.5	0.744±0.160
3	1/3	2694	3	898.0±518.2	1.672±0.969
	2/3	5292	2	2646.0±1870.7	0.629±0.445
4	1/3	4197	3	1399.0±807.4	1.073±0.622
	2/3	8144	2	4072.0±2879.0	0.409±0.289
5	1/3	29986	12	2498.8±721.2	0.601±0.175
	2/3	60057	24	2502.4±510.7	0.665±0.137
6	1/3	4069	3	1356.3±782.8	1.107±0.641
	2/3	8189	3	2729.7±1575.7	0.610±0.353
7	1/3	24574	6	4095.7±1671.8	0.366±0.150
	2/3	49636	19	2612.4±599.2	0.637±0.147
8	1/3	353	0	353.0±352.5	4.261±4.272
	2/3	629	0	629.0±628.5	2.649±2.652
9	1/3	23806	10	2380.6±752.7	0.630±0.201
	2/3	47603	21	2266.8±494.5	0.734±0.162
10	1/3	11037	4	2759.2±1379.4	0.544±0.273
	2/3	22037	10	2203.7±696.7	0.755±0.240
11	1/3	46	0	46.0±45.5	33.333±33.737
	2/3	61	0	61.0±60.5	27.725±27.968
12	1/3	26398	10	2639.8±834.6	0.568±0.182
	2/3	52787	23	2295.1±478.5	0.725±0.153
13	1/3	3214	3	1071.3±618.2	1.401±0.812
	2/3	6223	2	3111.5±2199.8	0.535±0.379

Table 4: The rejection branch for the $K_{\pi 2}$ TG scatter background in the loose box: PV rejection using the loose photon veto (PV60) for the $\pi\nu\overline{\nu}(2)$ box and the resulting background. The same setup cuts as in the loose normalization branch (Table 8) are applied.

Tight Rejection Branch - Loose PNN2 Box + PV30

CLASS		bef. PV	af. PV	PV Rejection	Background
2	1/3	24466	3	8155.3±4708.2	0.092±0.054
	2/3	49183	11	4471.2±1348.0	0.168±0.051
3	1/3	2694	1	2694.0±2693.5	0.280±0.280
	2/3	5292	2	2646.0±1870.7	0.284±0.201
4	1/3	4197	0	4197.0±4196.5	0.179±0.180
	2/3	8144	2	4072.0±2879.0	0.185±0.131
5	1/3	29986	4	7496.5±3748.0	0.100±0.051
	2/3	60057	12	5004.8±1444.6	0.150±0.044
6	1/3	4069	1	4069.0±4068.5	0.185±0.185
	2/3	8189	2	4094.5±2894.9	0.184±0.130
7	1/3	24574	1	24574.0±24573.5	0.031±0.031
	2/3	49636	8	6204.5±2193.4	0.121±0.043
8	1/3	353	0	353.0±352.5	2.139±2.146
	2/3	629	0	629.0±628.5	1.197±1.199
9	1/3	23806	3	7935.3±4581.2	0.095±0.055
	2/3	47603	11	4327.6±1304.7	0.174±0.053
10	1/3	11037	1	11037.0±11036.5	0.068±0.068
	2/3	22037	3	7345.7±4240.7	0.102±0.059
11	1/3	46	0	46.0±45.5	16.733±16.952
	2/3	61	0	61.0±60.5	12.525±12.642
12	1/3	26398	4	6599.5±3299.5	0.114±0.058
	2/3	52787	11	4798.8±1446.7	0.157±0.048
13	1/3	3214	1	3214.0±3213.5	0.234±0.235
	2/3	6223	2	3111.5±2199.8	0.242±0.171

Table 5: The rejection branch for the $K_{\pi 2}$ TG scatter background in the tight box: PV rejection using the tight photon veto (PV30) for the $\pi\nu\overline{\nu}(2)$ box and the resulting background. The same setup cuts as in the tight normalization branch (Table 9) are applied.

the systematic uncertainty.

Due to the loss of statistics in the rejection branch for the tight box [1], the rejection of the tight (30%) photon veto is measured on a rejection branch that uses the loose versions of the kinematic box, the TD cuts and DELCO. In doing this it is assumed that the rejection of the (30%) photon veto on these classes is the same for the loose and tight cuts. Tables 6 and 7 show that the rejection does not change within statistical error when applying the tight versions of these cuts to the 1/3 and 2/3 data sets respectively. Tables 11 and 12 summarize the photon veto rejections and other values used in the background estimation.

3.1.2 Normalization Branch

In the normalization branch (see Tables 8, 9 and 10), all the cuts in TGCUT06 were applied, and the PV was inverted. Some contamination from $K_{\pi 2}$-RS scatters and $K_{\pi 2\gamma}$ is expected, but these backgrounds are small compared to $K_{\pi 2}$-TG scatters. The ptot distribution of the events remaining in the normalization branch after the inversion of PVCUTPNN2, after the application of all the TGCUT06 except CCDPUL, and after the application of CCDPUL is shown in Figure 6. In the same figure, the ptot distribution of the events in class 12 of the rejection branch is also shown before and after PVCUTPNN2. Both of those distributions look adequately $K_{\pi 2}$-scatter-like. Table xxx summarizes the normalization values used for the background estimation.

3.1.3 Background

The $K_{\pi 2}$ target scatter background for the loose box $n_{K_{\pi 2}-TGscat}(\text{loose})$ is given by

$$n_{K_{\pi 2}-TGscat}(\text{loose}) \;=\; \frac{N}{R_{PV(60\%)} - 1} \tag{1}$$

, where the results from the 1/3 and 2/3 data sets are scaled to give results for the entire data set. The systematic error comes from the difference in background predicted by the class with the highest and lowest PV rejection, with respect to the central value from CLASS12. Only classes with adequate statistics are considered. The classes chosen for these systematic error bounds are shown in Tables 11 and 12.

For the tight box, the inverted photon veto used in the normalization branch was the loose (60%) photon veto as to not look in the box. Thus the the rejection branch required the use of the loose photon veto and the entire background was scaled by the ratio of the loose and tight (30%) photon vetoes. The tight $K_{\pi 2}$ target scatter background $n_{K_{\pi 2}-TGscat}(\text{tight})$ is given by

$$n_{K_{\pi 2}-TGscat}(\text{tight}) \;=\; \frac{N}{R_{PV(60\%)} - 1}\left(\frac{R_{PV(60\%)}}{R_{PV(30\%)}}\right), \tag{2}$$

where the results from the 1/3 and 2/3 data sets are scaled to give results for the entire data set. The lower and upper bounds on the systematic error again come from the

[1] Here, the tight box refers to the application of the tight KIN, TD and DELCO cuts

PV30 Rejection - 1/3 Sample

CLASS	All Loose	Ke4 Box	DELCO6	TDTIGHT	All Tight
2	24466/3 = 8155.33±4708.2	18377/3 = 6125.67±3536.4	21065/1 = 21065±21064.5	18259/1 = 18259±18258.5	11798/0 = 11798±11797.5
3	2694/1 = 2694±2693.5	2070/1 = 2070±2069.5	2162/1 = 2162±2161.5	2034/0 = 2034±2033.5	1250/0 = 1250±1249.5
4	4197/0 = 4197±4196.5	3243/0 = 3243±3242.5	3712/0 = 3712±3711.5	3119/0 = 3119±3118.5	2108/0 = 2108±2107.5
5	29986/4 = 7496.5±3748	22617/4 = 5654.25±2826.9	26121/2 = 13060.5±9234.8	22348/2 = 11174±7900.9	14663/1 = 14663±14662.5
6	4069/1 = 4069±4068.5	3167/1 = 3167±3166.5	3294/1 = 3294±3293.5	3064/0 = 3064±3063.5	1924/0 = 1924±1923.5
7	24574/1 = 24574±24573.5	18632/1 = 18632±18631.5	21929/1 = 21929±21928.5	18317/1 = 18317±18316.5	12376/1 = 12376±12375.5
8	353/0 = 353±352.5	294/0 = 294±293.5	302/0 = 302±301.5	252/0 = 252±251.5	185/0 = 185±184.5
9	23806/3 = 7935.33±4581.2	17903/3 = 5967.67±3445.1	20379/1 = 20379±20378.5	17713/1 = 17713±17712.5	11397/0 = 11397±11396.5
10	11037/1 = 11037±11036.5	7981/1 = 7981±7980.5	9876/1 = 9876±9875.5	8211/1 = 8211±8210.5	5292/1 = 5292±5291.5
11	46/0 = 46±45.5	41/0 = 41±40.5	37/0 = 37±36.5	32/0 = 32±31.5	23/0 = 23±22.5
12	26398/4 = 6599.5±3299.5	19802/4 = 4950.5±2475	22846/2 = 11423±8076.9	19688/2 = 9844±6960.4	12761/1 = 12761±12760.5
13	3214/1 = 3214±3213.5	2433/1 = 2433±2432.5	2566/1 = 2566±2565.5	2410/0 = 2410±2409.5	1449/0 = 1449±1448.5

Table 6: Rejection of the tight (30%) photon veto for the 1/3 sample for the various classes with different combinations of loose and tight versions of the setup cuts: kinematic box cut, TD cuts and DELCO. The "All Loose" and "All Tight" columns mean that those three sets of cuts were all loose or all tight. For the other three columns, all the cuts are loose except the one listed, which is tight. The numbers shown are the number of events before the photon veto is applied divided by the number of events remaining after the photon veto is applied and the resulting rejection with statistical error. If there are zero events remaining after the photon veto is applied, the rejection is determined assuming 1 event remained. Note that the events remaining after the photon veto has been applied from all classes in the "All Loose" column are a sub-set of the events from class 12. The kinematics of these four events have been confirmed to have kinematics that would put them in the ke4-phobic kinematic box.

PV30 Rejection - 2/3 Sample

CLASS	All Loose	Ke4 Box	DELCO6	TDTIGHT	All Tight
2	49183/11 = 4471.18±1348	36895/10 = 3689.5±1166.6	42357/8 = 5294.63±1871.8	36729/8 = 4591.13±1623	23665/6 = 3944.17±1610
3	5292/2 = 2646±1870.7	4025/2 = 2012.5±1422.7	4225/2 = 2112.5±1493.4	3981/1 = 3981±3980.5	2430/1 = 2430±2429.5
4	8144/2 = 4072±2879	6260/1 = 6260±6259.5	7284/0 = 7284±7283.5	6064/2 = 3032±2143.6	4124/0 = 4124±4123.5
5	60057/12 = 5004.75±1444.6	45161/11 = 4105.55±1237.7	52361/8 = 6545.13±2313.9	44850/9 = 4983.33±1660.9	29318/6 = 4886.33±1994.6
6	8189/2 = 4094.5±2894.9	6318/2 = 3159±2233.4	6665/2 = 3332.5±2356.1	6203/1 = 6203±6202.5	3912/1 = 3912±3911.5
7	49636/8 = 6204.5±2193.4	37524/7 = 5360.57±2025.9	44381/4 = 11095.3±5547.4	37010/7 = 5287.14±1998.2	24929/4 = 6232.25±3115.9
8	629/0 = 629±628.5	498/0 = 498±497.5	549/0 = 549±548.5	475/0 = 475±474.5	331/0 = 331±330.5
9	47603/11 = 4327.55±1304.7	35537/11 = 3230.64±973.9	40857/8 = 5107.13±1805.5	35608/8 = 4451±1573.5	22741/6 = 3790.17±1547.1
10	22037/3 = 7345.67±4240.7	15971/2 = 7985.5±5646.2	19757/2 = 9878.5±6984.8	16501/3 = 5500.33±3175.3	10710/2 = 5355±3786.2
11	61/0 = 61±60.5	49/0 = 49±48.5	51/0 = 51±50.5	43/0 = 43±42.5	30/0 = 30±29.5
12	52787/11 = 4798.82±1446.7	39607/10 = 3960.7±1252.3	45721/8 = 5715.13±2020.4	39416/8 = 4927±1741.8	25550/6 = 4258.33±1738.2
13	6223/2 = 3111.5±2199.8	4672/2 = 2336±1651.4	4988/2 = 2494±1763.2	4671/1 = 4671±4670.5	2831/1 = 2831±2830.5

Table 7: Rejection of the tight (30%) photon veto for the 2/3 sample for the various classes with different combinations of loose and tight versions of the setup cuts: kinematic box cut, TD cuts and DELCO. The "All Loose" and "All Tight" columns mean that those three sets of cuts were all loose or all tight. For the other three columns, all the cuts are loose except the one listed, which is tight. The numbers shown are the number of events before the photon veto is applied divided by the number of events remaining after the photon veto is applied and the resulting rejection with statistical error. If there are zero events remaining after the photon veto is applied, the rejection is determined assuming 1 event remained. Note that the events remaining after the photon veto has been applied from all classes in the "All Loose" column are a sub-set of the events from class 12. The kinematics of these four events have been confirmed to have kinematics that would put them in the ke4-phobic kinematic box.

Loose Normalization Branch

CUT	1/3	2/3
ALL_EVENTS	92709448	92709448
BAD_RUN,KERROR	90192888	90192888
SKIM2/5,RECON	2635077	5264890
PSCUT06	952180	1905107
DELCO3	945357	1891173
TDCUT02 loose	711847	1423458
KINCUT06	417199	833241
PNN2 KIN BOX loose	38835 (10.743)	77831 (10.706)
$\overline{\text{PV60}}$	38820 (1.000)	77795 (1.000)
B4EKZ(IC)	27787 (1.397)	55768 (1.395)
TGZFOOL	27396 (1.014)	55032 (1.013)
EPITG	17250 (1.588)	34859 (1.579)
EPIMAXK	17250 (1.000)	34859 (1.000)
TARGF	14700 (1.173)	29677 (1.175)
DTGTTP	14700 (1.000)	29677 (1.000)
RTDIF	14590 (1.008)	29424 (1.009)
DRP	14388 (1.014)	28982 (1.015)
TGKTIM	14144 (1.017)	28482 (1.018)
EIC	13847 (1.021)	27843 (1.023)
TIC	13847 (1.000)	27843 (1.000)
TGEDGE	13621 (1.017)	27394 (1.016)
TGDEDX	12809 (1.063)	25918 (1.057)
TGENR	12533 (1.022)	25403 (1.020)
PIGAP	12342 (1.015)	25037 (1.015)
TGB4	11082 (1.114)	22562 (1.110)
KIC	11076 (1.001)	22556 (1.000)
PHIVTX	8289 (1.336)	16873 (1.337)
OPSVETO	7238 (1.145)	14793 (1.141)
TGLIKE	6812 (1.063)	13863 (1.067)
TIMKF	5542 (1.229)	11358 (1.221)
NPITG	5542 (1.000)	11358 (1.000)
ALLKFIT	5295 (1.047)	10857 (1.046)
TPICS	5291 (1.001)	10856 (1.000)
EPIONK	4970 (1.065)	10204 (1.064)
CHI567	4143 (1.200)	8514 (1.198)
VERRNG	3455 (1.199)	7055 (1.207)
CHI5MAX	3454 (1.000)	7055 (1.000)
ANGLI	3445 (1.003)	7039 (1.002)
CCDBADFIT	3083 (1.117)	6214 (1.133)
CCDBADTIM	2991 (1.031)	6026 (1.031)
CCD31FIB	2991 (1.000)	6026 (1.000)
CCDPUL	500 (5.982)	1109 (5.434)

Table 8: The normalization branch for the loose $K_{\pi 2}$-TG scatter background: events after setup cuts and TGCUTS and their rejection (in brackets) in the $\pi\nu\overline{\nu}(2)$ loose box.

Tight Normalization Branch

CUT	1/3	2/3
ALL_EVENTS	92709448	92709448
BAD_RUN,KERROR	90192888	90192888
SKIM2/5,RECON	2635077	5264890
PSCUT06	952180	1905107
DELCO6	778661	1560187
TDCUT02 tight	428074	858447
KINCUT06	257607	516539
Ke4-phobic KIN BOX	18911 (13.622)	37733 (13.689)
$\overline{\text{PV60}}$	18907 (1.000)	37714 (1.000)
B4EKZ(IC)	13617 (1.388)	27008 (1.396)
TGZFOOL	13437 (1.013)	26631 (1.014)
EPITG	8228 (1.633)	16470 (1.617)
EPIMAXK	8228 (1.000)	16470 (1.000)
TARGF	6914 (1.190)	13831 (1.191)
DTGTTP	6914 (1.000)	13831 (1.000)
RTDIF	6870 (1.006)	13720 (1.008)
DRP	6791 (1.012)	13565 (1.011)
TGKTIM	6761 (1.004)	13502 (1.005)
EIC	6623 (1.021)	13237 (1.020)
TIC	6623 (1.000)	13237 (1.000)
TGEDGE	6535 (1.013)	13079 (1.012)
TGDEDX	6120 (1.068)	12360 (1.058)
TGENR	5988 (1.022)	12102 (1.021)
PIGAP	5883 (1.018)	11909 (1.016)
TGB4	5251 (1.120)	10663 (1.117)
KIC	5248 (1.001)	10660 (1.000)
PHIVTX	3826 (1.372)	7767 (1.372)
OPSVETO	3374 (1.134)	6872 (1.130)
TGLIKE	3176 (1.062)	6426 (1.069)
TIMKF	2621 (1.212)	5357 (1.200)
NPITG	2621 (1.000)	5357 (1.000)
ALLKFIT	2507 (1.045)	5131 (1.044)
TPICS	2504 (1.001)	5130 (1.000)
EPIONK	2321 (1.079)	4727 (1.085)
CHI567	1898 (1.223)	3857 (1.226)
VERRNG	1592 (1.192)	3168 (1.217)
CHI5MAX	1591 (1.001)	3168 (1.000)
ANGLI	1588 (1.002)	3161 (1.002)
CCDBADFIT	1426 (1.114)	2775 (1.139)
CCDBADTIM	1381 (1.033)	2692 (1.031)
CCD31FIB	1381 (1.000)	2692 (1.000)
CCDPUL	251 (5.502)	501 (5.373)

Table 9: The normalization branch for the tight $K_{\pi 2}$-TG scatter background: events after setup cuts and TGCUTS and their rejection (in brackets) in the $\pi\nu\overline{\nu}(2)$ ke4-phobic box. Note that it is the loose 60% photon veto that is inverted for the tight normalization branches.

Loose Normalization Branch in KP2 Kinematic Box

CUT	1/3	2/3
ALL_EVENTS	92709448	92709448
BAD_RUN,KERROR	90192888	90192888
SKIM2/5,RECON	2635077	5264890
PSCUT06	952180	1905107
DELCO3	945357	1891173
TDCUT02 loose	711847	1423458
KINCUT06	417199	833241
KP2 KIN BOX	337622 (1.236)	674203 (1.236)
$\overline{\text{PV60}}$	337377 (1.001)	673562 (1.001)
B4EKZ(IC)	307443 (1.097)	613750 (1.097)
TGZFOOL	302502 (1.016)	603827 (1.016)
EPITG	265780 (1.138)	529424 (1.141)
EPIMAXK	265780 (1.000)	529424 (1.000)
TARGF	256810 (1.035)	511730 (1.035)
DTGTTP	256803 (1.000)	511722 (1.000)
RTDIF	254618 (1.009)	507370 (1.009)
DRP	253746 (1.003)	505667 (1.003)
TGKTIM	251265 (1.010)	500819 (1.010)
EIC	247096 (1.017)	492280 (1.017)
TIC	247095 (1.000)	492275 (1.000)
TGEDGE	244792 (1.009)	487869 (1.009)
TGDEDX	243294 (1.006)	485094 (1.006)
TGENR	236833 (1.027)	472146 (1.027)
PIGAP	235171 (1.007)	468742 (1.007)
TGB4	221207 (1.063)	440987 (1.063)
KIC	221103 (1.000)	440790 (1.000)
PHIVTX	213725 (1.035)	425722 (1.035)
OPSVETO	204252 (1.046)	406804 (1.046)
TGLIKE	197703 (1.033)	393828 (1.033)
TIMKF	175933 (1.124)	350615 (1.123)
NPITG	175933 (1.000)	350615 (1.000)
ALLKFIT	169905 (1.035)	338574 (1.036)
TPICS	169877 (1.000)	338520 (1.000)
EPIONK	159031 (1.068)	316969 (1.068)
CHI567	138310 (1.150)	275107 (1.152)
VERRNG	129595 (1.067)	257769 (1.067)
CHI5MAX	129595 (1.000)	257769 (1.000)
ANGLI	129524 (1.001)	257629 (1.001)
CCDBADFIT	114548 (1.131)	227724 (1.131)
CCDBADTIM	112107 (1.022)	222903 (1.022)
CCD31FIB	112105 (1.000)	222903 (1.000)
CCDPUL	60473 (1.854)	120371 (1.852)

Table 10: The normalization branch for the $K_{\pi 2}$-TG scatter background in the KP2 box: events after setup cuts and TGCUTS and their rejection (in brackets) in the $K_{\pi 2}$ box.

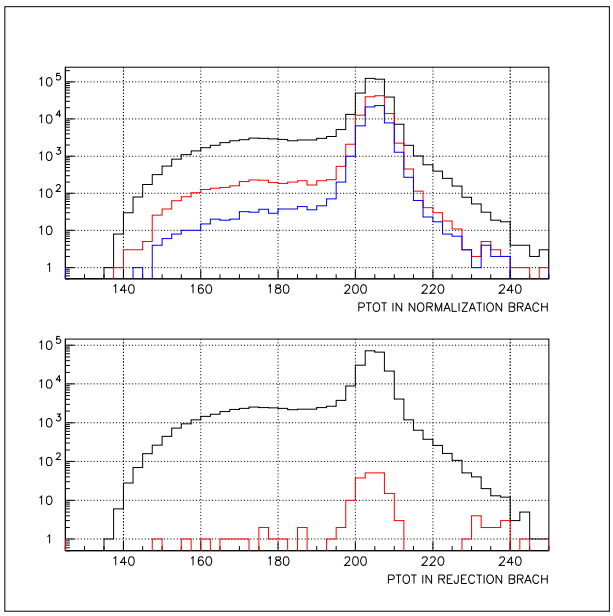

Figure 6: Top: ptot distribution of the events remaining in the normalization branch of the $K_{\pi 2}$ TG scatter study after the inversion of PVCUT (black), after the application of all the TGCUT06 except CCDPUL (red), and after the application of CCDPUL (blue). Bottom: ptot distribution of the events in CLASS12 of the rejection branch of the $K_{\pi 2}$ TG scatter study before (black) and after (red) PVCUT. (Note that these plots were made using 1/3 data.)

Loose $K_{\pi 2}$ Target Scatter Summary		
	1/3	2/3
Normalization		
N	500	1109
Photon Veto Rejection R_{PV60}		
R_{PV60}(CLASS12)	2639.8±834.6	2295.1±478.5
R_{PV60}(max.)	4095.7±1671.8 (CLASS7)	2612.4±599.2 (CLASS7)
R_{PV60}(min.)	2380.6±752.7 (CLASS9)	2203.7±696.7 (CLASS10)
R_{PV60}	$2639.8 \pm 834.6^{+1455.9}_{-259.2}$	$2295.1 \pm 478.5^{+317.3}_{-91.4}$
Background Estimate: $n_{\rm bg} = N/(R_{PV60} - 1)$		
$n_{\rm bg}$	$0.568 \pm 0.182^{+0.062}_{-0.202}$	$0.725 \pm 0.153^{+0.030}_{-0.088}$

Table 11: The summary of the loose $K_{\pi 2}$ target-scatter background estimation. For the photon veto rejection R_{PV60} and background estimate n_{bg}, the first error is statistical and the second error systematic. The maximum and minimum 60% photon veto rejections are labeled to show which class was used to determine the systematic errors in R_{PV60} and n_{bg}.

difference in background predicted by the class with the highest and lowest PV rejections with respect to CLASS12. Only classes with adequate statistics are considered. For the purposes of determining the bounds on the systematic error, the difference in photon veto rejection for CLASS12 between the "All Loose" and "Ke4-phobic kinematic box" setups cuts (Table 6 and 7) is treated as another class.

Tables 11 and 12 show the summary of all values used to determine these loose and tight backgrounds respectively.

3.2 $K^+ \to \pi^+\pi^o$ Range Stack Scatters

3.2.1 Background

Pions from the $K_{\pi 2}$ decay can also undergo inelastic scattering in the Range Stack and fall into the $\pi\nu\overline{\nu}(2)$ kinematic box by losing energy in the scattering process. However, for these events to be a background for this analysis, the pion momentum also has to be mis-measured and the photons from the π^o decay have to be missed. Therefore, this background is expected to be smaller compared to the $K_{\pi 2}$ target scattered background. It should be noted that these background events are already included in the normalization

Tight $K_{\pi 2}$ Target Scatter Summary

	1/3	2/3
	Normalization	
N	251	501
	Photon Veto Rejection R_{PV30}	
R_{PV30}(CLASS12)	6599.5±3299.5	4798.8±3299.5
R_{PV30}(max.)	8155.3±4708.2 (CLASS2)	6204.5±2193.4 (CLASS7)
R_{PV30}(min.)	4950.5±2475.0 (KE4-PHOBIC)	3960.7±1252.3 (KE4-PHOBIC)
R_{PV30}	$6599.5 \pm 3299.5^{+1555.8}_{-1649.0}$	$4798.8 \pm 1446.7^{+1405.7}_{-838.1}$
	Photon Veto Rejection R_{PV60}	
R_{PV60}[1]	$2639.8 \pm 834.6^{+1455.9}_{-259.2}$	$2295.1 \pm 478.5^{+317.3}_{-91.4}$
	Background Estimate: $n_{\rm bg} = \frac{N}{R_{PV60}-1}\left(\frac{R_{PV60}}{R_{PV30}}\right)$	
$n_{\rm bg}$	$0.114 \pm 0.058^{+0.038}_{-0.022}$	$0.157 \pm 0.048^{+0.033}_{-0.035}$

Table 12: The summary of the tight $K_{\pi 2}$ target-scatter background estimation. For the photon veto rejection R_{PV60} and background estimate n_{bg}, the first error is statistical and the second error systematic. The maximum and minimum 30% photon veto rejections are labeled to show which class was used to determine the systematic errors in R_{PV60} and n_{bg}. The rejection for the 60% photon veto is taken from Table 11

RS-Scat Rejection Branch - Loose Box

CUT	KP2BOX		KP2-PBOX PNN2-REBOX	
	1/3	2/3	1/3	2/3
PBOX from KP2BOX	92433	184549	718	1528
LAYER14	92380	184445	718	1528
FIDUCIAL	85219	170030	648	1378
UTCQUAL	82535	164571	635	1331
RNGMOM	81833	163202	635	1331
RSDEDX	71445	142564	113	266
PRRF	60508	120477	81	190
PVCUT	35	106	0	0

Table 13: The loose rejection branch for $K_{\pi 2}$-RS scatters. PBOX is the momentum cut and RE BOX the range and energy cut.

branches in Tables 8 and 9[2], but they are not included in the rejection branch in Table 4 because the target cuts were reversed to measure this PV rejection. The $K_{\pi 2}$ events which scattered in the RS should be assigned the same Photon Veto rejection as the $K_{\pi 2}$ peak events, since the pion did not scatter in the target. The method used to determine this background was originally formulated by Milind et al. [2].

The most effective cuts against this background are the Range Stack track quality cuts RSDEDX and PRRF (collectively referred to as RSCT), the BOX cut on *ptot* and the Photon Veto cut. The SETUP cuts are the same as the $K_{\pi 2}$ target scatter normalization branch. Tables 13 and 14 contain events in the $K_{\pi 2}$ momentum peak. Events with the momentum of the $K_{\pi 2}$ peak events, but lowered in range and energy are assumed to have scattered in the Range Stack.

The efficiency ϵ_{RSCT} and the rejection R_{RSCT} of the RSCT cuts can be determined from the RS-Scatter Rejection Tables 13 and 14. The efficiency ϵ_{RSCT} is determined from the "KP2BOX" column and the rejection R_{RSCT} from the "KP2-PBOX PNN2-REBOX" column.

$$\epsilon_{RSCT} = N_{\rm PRRF}/N_{\rm RNGMOM} \quad (3)$$

$$R_{RSCT} = N_{\rm RNGMOM}/N_{\rm PRRF} \quad (4)$$

Tables 15 and 16 show the normalization branch. The RSCT cut is reversed and all other cuts are applied. The various contributions to the total *norm_rs* events left at the the end of the branch have to be considered in order to calculate the background of interest. The largest component of this sample comes from scattering in the target that contaminated the RSCT reversed sample because of the inefficiency of the RSCT cuts. On the other hand, the total *norm_tg* events left at the end of the $K_{\pi 2}$ target scatter

[2]Correcting the normalization of $K_{\pi 2}$-TG scatters for $K_{\pi 2}$-RS scatters does not make a significant difference in the background, given the statistical uncertainty.

RS-Scat Rejection Branch - Tight Box

CUT	KP2BOX		KP2-PBOX KE4-PHOBIC REBOX	
	1/3	2/3	1/3	2/3
PBOX from KP2BOX	61499	123115	344	824
LAYER14	61465	123048	344	824
FIDUCIAL	56753	113485	307	753
UTCQUAL	54957	109853	302	726
RNGMOM	54484	108963	302	726
RSDEDX	47689	95486	63	167
PRRF	40549	80990	44	119
PVCUT	11	35	0	0

Table 14: The tight rejection branch for $K_{\pi 2}$-RS scatters. PBOX is the momentum cut and RE BOX the range and energy cut.

RS-Scat Normalization Branch - Loose Box

CUT	KP2BOX		PNN2BOX	
	1/3	2/3	1/3	2/3
$\overline{\text{RSDEDX}}$.or.$\overline{\text{PRRF}}$	24929	49809	217	402
LAYER14	24909	49771	217	402
FIDUCIAL	22448	44997	202	380
UTCQUAL	21545	43191	179	344
RNGMOM	21325	42725	153	278
$\overline{\text{PVCUT60}}$	21316	42699	153	278

Table 15: The loose normalization branch for $K_{\pi 2}$-RS scatters.

RS-Scat Normalization Branch - Tight Box

CUT	KP2BOX		KE4-PHOBIC BOX	
	1/3	2/3	1/3	2/3
$\overline{\text{RSDEDX}}$.or.$\overline{\text{PRRF}}$	16309	32664	81	153
LAYER14	16297	32640	81	153
FIDUCIAL	14696	29449	75	147
UTCQUAL	14089	28276	68	132
RNGMOM	13935	27973	66	120
$\overline{\text{PVCUT60}}$	13928	27959	66	120

Table 16: The tight normalization branch for $K_{\pi 2}$-RS scatters.

$K_{\pi 2}$ Range Stack Scatter Summary

	Loose		Tight	
	1/3	2/3	1/3	2/3
	$\epsilon_{RSCT} = N_{\rm PRRF}/N_{\rm RNGMOM}$			
$N_{\rm PRRF}$	60508	120477	40549	80990
$N_{\rm RNGMOM}$	81833	163202	54484	108963
ϵ_{RSCT}	0.739±0.002	0.738±0.001	0.744±0.002	0.743±0.001
	$R_{RSCT} = N_{\rm RNGMOM}/N_{\rm PRRF}$			
$N_{\rm RNGMOM}$	635	1331	302	726
$N_{\rm PRRF}$	81	190	44	119
R_{RSCT}	7.840±0.814	7.005±0.471	6.864±0.956	6.101±0.511
	Normalization Numbers			
$norm\_tg$	500	1109	251	501
$norm\_rs$	153	278	66	120
N_{rs}	-3.579±2.305	-20.402±3.995	-3.670±1.882	-11.153±3.064
	Photon Veto Rejection R_{PV60} ($K_{\pi 2}$ peak)			
Before PV	60508	120477	40549	80990
After PV	35	106	11	35
R_{PV60}	1728.8±292.1	1136.6±110.3	3686.3±1111.3	2314.0±391.1
	$n_{\rm bg} = N_{rs}/(R_{PV60} - 1)$			
$n_{\rm bg}$	-0.0062±0.0041	-0.0269±0.0059	-0.0030±0.0018	-0.0072±0.0023

Table 17: The summary of the $K_{\pi 2}$ range-stack scatter background estimation.

normalization branch (Tables 8 and 9) have a target scattered (N_{tg}) and a RS scattered (N_{rs}) component. We can write

$$N_{tg} + N_{rs} = norm\_tgnonumber \quad (5)$$

$$\frac{1-\epsilon_{RSCT}}{\epsilon_{RSCT}} \times N_{tg} + (R_{RSCT} - 1) \times N_{rs} = norm\_rs \quad (6)$$

Note that the form of the second equation has been corrected from that as used by Milind et al. [2]. As seen in Table 17, solving this system of equations gives negative solutions for the range stack scattered component N_{rs} for both the loose and tight boxes in the 1/3 and 2/3 data sets.

The final background from the RS scattered events can be determined from N_{rs} and the $K_{\pi 2}$ peak Photon Veto rejection from CLASS1 as shown:

$$n_{K_{\pi 2}-RSscat} = \frac{N_{rs}}{R_{PV-K_{\pi 2}peak} - 1} \quad (7)$$

where a normalization factor of 3 is used for the 1/3 data sample and a normalization factor of 3/2 for the 2/3 data sample.

3.2.2 Effect of $K_{\pi 2}$-range-tail Contamination

The range stack scattered component N_{rs} as determined by Equations 6 is most sensitive to small relative changes in the efficiency ϵ_{RSCT}. This efficiency is measured on $K_{\pi 2}$-peak events under the assumption that these events will have decay pions that look the most like pions from target-scatters and will not scatter in the range stack. The rejection of these cuts is measured on the pion range-tail which runs right up to the $K_{\pi 2}$-peak. The contamination of pion range-tail events in the $K_{\pi 2}$-peak sample results in the calculated efficiency being too low.

To better isolate these true $K_{\pi 2}$-peak events from the pion range-tail events, two additional $K_{\pi 2}$-peak kinematic boxes were created, the "Tight" and "Super-tight" $K_{\pi 2}$ kinematic boxes. The bounds on momentum, energy and range for the regular, "Tight" and "Super-tight" $K_{\pi 2}$ kinematic boxes are shown in Table 18. The table shows that resulting background from the "Super-tight" box for the loose 2/3 sample is still over 3 sigma from being equal to 0 within statistical error. Due to resolution effects, even the "Super-tight" box is contaminated with pion range-tail events. It can be argued that extrapolating the results from Table 18 to a sample of pure $K_{\pi 2}$-peak events would result in a value of ϵ_{RSCT} that is large enough such that the $K_{\pi 2}$ range-stack scatter background for both the 1/3 and 2/3 samples to equal to zero within statistical error. Thus the $K_{\pi 2}$ range-stack scatter background can be considered negligible.

4 $K_{\pi 2\gamma}$ Background

Needs to be written for 2/3 analysis.

	Regular	Tight	Super-Tight
PTOT	199-215	202-210	203-209
RTOT	28-35	29-32	29.4-31.6
ETOT	100.5-115	100.5-110	101-108
$\epsilon_{RSCT}(LooseSetup)$	0.739 ± 0.002	0.758 ± 0.002	0.759 ± 0.003
Background(Loose,1/3)	-0.0062 ± 0.0041		-0.0015±0.0038
Background(Loose,2/3)	-0.0269 ± 0.0059		-0.0176±0.0051

Table 18: Bounds of the $K_{\pi 2}$-peak kinematic boxes used to measure the effects of pion range-tail contamination on ϵ_{RSCT}. The resulting $K_{\pi 2}$ range-stack scatter background is excluded for the 'Tight' box since it is nearly identical to the result for the 'Super-tight' box.

5 Beam Background

The statistics of the beam background samples are very limited. Efforts went into obtaining comparatively higher statistic samples by loosing cuts. Within all beam background studies, 1-beam and 2-beam, the PV was applied with the same cut parameters as was performed in PNN1; applying PV_{pnn2} will remove all events well before all other cuts are applied. Therefore, we must scale by $\frac{A_{PV_{pnn2}}}{A_{PV_{pnn1}}}$ where $A_{PV_{pnn1}} = 0.925$ and $A_{PV_{pnn2}} = 0.639$ for the loose signal region and $A_{PV_{pnn2}} = 0.356$ for the tight region. The value for $A_{PV_{pnn1}} = 0.925$ was measured with the PNN2 setup cuts, as shown in Table **??**. Also, note that the acceptances shown here ($A_{PV_{pnn2}}, A_{PV_{pnn1}}$) are the PV subsystems which are included in pvcut02_new.function (TG, IC,VC,CO,MC,EC,RD,BV,BVL for both pnn1 and pnn2 and also including ADPV, earlyBV, DS,earlyBVL for pnn2). Scaling by the PV acceptance-loss is justified by beam backgrounds being independent upon the PV cuts (except for ADPV on the 2-beam). That is, there is no expectation of additional rejection against these background for the PV cuts (except for the ADPV cut in the 2-beam background which is discussed in Section 5.2).

For comparison, the beam background is explicitly measured in the tight region in the following sections. However, PNN2 will be utilizing the value from scaling the background in the loose region. Further, details of the beam background were written in Ref. [5].

5.1 Single-Beam Background

The single-beam background is bifurcated with DELCO. In the normalization brach, we invert the loosest version of DELCO which is DELC3. This is to preserve the blind analysis. The rejection branch as shown in Fig. 7 has three branches. This follows what was done in PNN1; higher statistics samples were obtained by not applying kinematic (KIN) and/or TD cuts. Due to the 1 beam background being relatively small compared to the other beam backgrounds (and very small compared to Kpi2 scattering) a conservative estimate was chosen, i.e. the cleanest sample (with TD*KIN applied) with the lowest

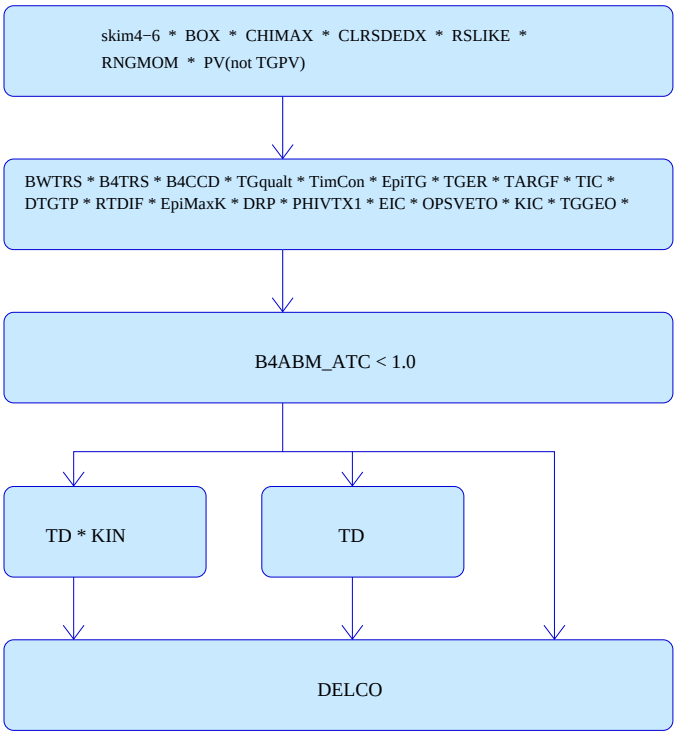

Figure 7: **1-Beam Rejection Bifurcation**. The additional branches in this rejection bifurcation is cleaning up the sample with additional cuts at the expense of reducing statistics. *DELCO*=DEL3 OR DELC6 depending on what signal region is being studied.

statistics was used in the final measurement.

$$N_{1bm} = 3 \times \frac{A_{PV_{pnn2}}}{A_{PV_{pnn1}}} \times \frac{N_{1bm}}{R_{delco} - 1} \tag{8}$$

$$\begin{aligned} N_{1bm_{loose}} &= 3 \times \frac{0.639}{0.925} \times \frac{5.0 \pm 2.2}{(6398.0 \pm 6397.5) - 1} \\ &= (1.58 \pm 1.58) \times 10^{-3} \end{aligned} \tag{9}$$

$$\begin{aligned} N_{1bm_{tight}} &= 3 \times \frac{0.356}{0.925} \times \frac{2.0 \pm 1.4}{(3857.0 \pm 3856.5) - 1} \\ &= (1.58 \pm 1.58) \times 10^{-3} \end{aligned} \tag{10}$$

If we "measure" the tight value from scaling from 1-beam loose value, we obtain the following: Note that the factor of 3 is included in the value of $N_{1bm_{loose}}$.

$$N^{scaled}_{1bm_{tight}} = \frac{A_{PV_{tight}}}{A_{PV_{loose}}} \times \frac{A_{TD_{tight}}}{A_{TD_{loose}}} \times \frac{A_{BOX_{tight}}}{A_{BOX_{loose}}} \times \frac{A_{DELCO_{tight}}}{A_{DELCO_{loose}}} \times N_{1bm_{loose}} \tag{11}$$

$$\begin{aligned} N^{scaled}_{1bm_{tight}} &= \frac{0.356}{0.639} \times \frac{0.704}{0.942} \times (0.68) \times \frac{0.704}{0.857} \times 0.00157 \\ &= (0.35 \pm 0.35) \times 10^{-3} \end{aligned} \tag{12}$$

Setup Branch	$1/3\ Rej^{loose}_{DELCO}$	$1/3\ Rej^{tight}_{DELCO}$	$2/3\ Rej^{loose}_{DELCO}$
Loose Setup	10590.0 ± 7487.9 (2)	17800.0 ± 17799.5 (1)	3190.8 ± 884.8 (13)
TD	17625.0 ± 17624.5 (1)	10743.0 ± 10742.5 (1)	4931.3 ± 1863.7 (7)
TD · KIN	$\mathbf{6398.0 \pm 6397.5}$ **(1)**	$\mathbf{3857.0 \pm 3856.5}$ **(1)**	$\mathbf{6179.5 \pm 4369.2}$ **(2)**

Table 19: **1-Beam Rejection Summary**. Each row is a different branch to measure the DELCO rejection with samples becoming cleaner for each subsequent row. First number is the rejection. The number is parenthesis is the number of events remaining that the rejection is based upon. The minimum rejection is used in calculation of the 1-BM background for a conservative estimate.

	$1/3\ Norm^{loose}_{1bm}$	$1/3\ Norm^{tight}_{1bm}$	$2/3\ Norm^{loose}_{1bm}$
$\overline{DELC3}$	5.0 ± 2.2	2.0 ± 1.4	23.0 ± 4.8

Table 20: **1-Beam Normalization Summary** In the 1-bm normalization, DECL3 was inverted for both the loose and tight regions. PV_{pnn1} was applied as a loose PV cut instead of the loose and tight versions of PV_{pnn2}.

$N^{scaled}_{1bm_{tight}}$ is consistent with $N_{1bm_{tight}}$. If we use the $Rej_{delco} = 6239$ from the loose region (which has more statistics) for the tight region then $N_{1bm_{tight}} = 0.33 \times 10^{-3}$.

5.2 Double-Beam Background

The normalization of double-beam background measurement was modified since Ref. [5]. Previously, ADPV was not applied as a cut, since PV_{pnn1} was applied which did not include ADPV. For PNN2, a correction for the difference between PNN1 and PNN2 Photon Veto was applied by multiplying by the ratio of the acceptance of these two cuts. However, ADPV is known to have rejection above acceptance loss for 2-beam background. Therefore, previous studies overestimated the 2-beam background due to the additional rejection of ADPV. The solution that was devised to solve this issue was to change the bifurcation of the double beam (KK and Kpi) branches, see bottom of Fig. 8(b). This also reduced an previous issue with correlation of the B4 and TG cuts which were the cuts which were bifurcated previously. The ADPV should be less correlated with the B4 and TG compared to the bifurcation strategy employed in E949-PNN1 [6].

Scale by acceptance by $PV_{no\ AD}$ due to applying ADPV in the normalization branch. $PV_{no\ AD}$ is 0.673 (0.673) for loose (tight) which is determined by Table **??**. Table 21 corresponds to Fig. 8(a) and Table 22 corresponds to Fig. 8(b).

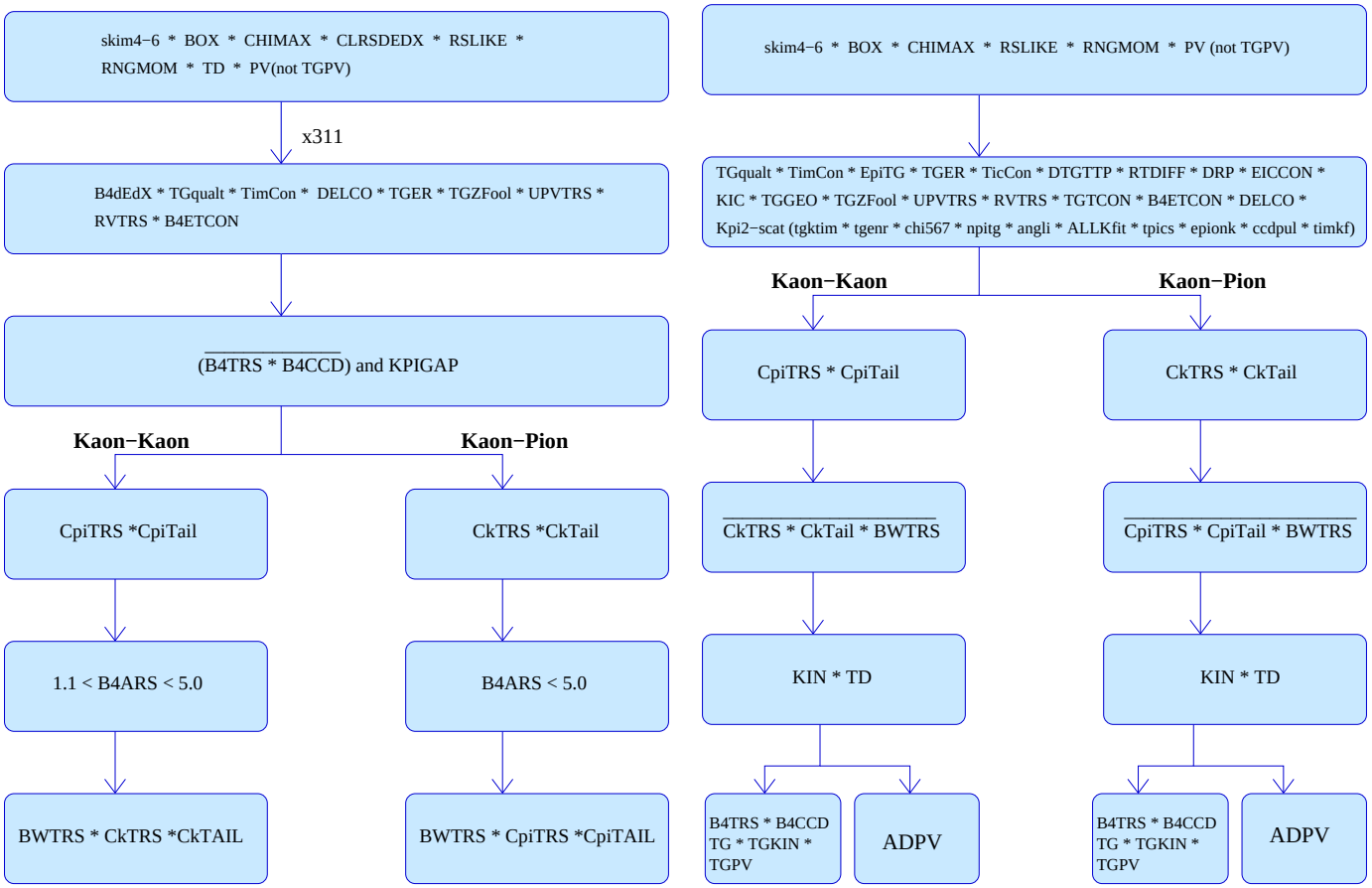

(a) Rejection (b) Normalization

Figure 8: **2-Beam Bifurcations (Kaon-Kaon and Kaon-Pion).** *DELCO* changes depending on the study. *DELCO*=DEL3 OR DELC6 depending on what signal region is being studied.

Rejection of	$1/3\ Rej_{KK}^{loose}$	$2/3\ Rej_{KK}^{tight}$	$2/3\ Rej_{KK}^{loose}$
$R_{KK}:\ BWTRS \cdot CkTRS \cdot CkTail$	61.9 ± 9.8 (39)	59.9 ± 12.7 (22)	54.3 ± 5.8 (86)
$R_{Kpi}:\ BWTRS \cdot CpiTRS \cdot CpiTail$	352.5 ± 124.5 (8)	274.3 ± 111.8 (6)	264.9 ± 57.7 (21)

Table 21: **2-Beam Rejection Summary**. First number is the rejection. The number in parenthesis is the number of events remaining that the rejection is based upon. K-K is the case where two Kaons are entering the beam. K-pi is the case where we have a Kaon and a Pion entering. $\overline{B4TRS \cdot B4CCD}\ AND\ KPIGAP$ is applied to select the rejection sample. KIN, TD and many other cuts listed in these flow charts are composite cuts.

Norm. branches	1/3 loose	1/3 tight	2/3 loose
$n_{KK}:\ TG \cdot TGPV \cdot B4$	8.0 ± 2.8	1.0 ± 1.0	19.0 ± 4.36
$r_{KK}:\ ADPV$	7.3 ± 2.6	7.3 ± 3.9	$5.41\pm$
N_{KK}	1.1 ± 0.55	0.136 ± 0.136	$3.51\pm$
$n_{Kpi}:\ TG \cdot TGPV \cdot B4$	10.0 ± 3.2	3.0 ± 1.7	3.0 ± 1.73
$r_{Kpi}:\ ADPV$	21.0 ± 10.2	45.0 ± 44.5	$6.84\pm$
N_{Kpi}	0.5 ± 0.3	0.1 ± 0.1	$0.438\pm$

Table 22: **2-Beam Normalization Summary**. The 2-BM Normalization has 2 branches that are further bifurcated. $K\text{-}K_{r,n}$, $K\text{-}pi_{r,n}$ are the results of the bifurcations, r=rejection, n=normalization, which we used to determine the last two rows. N_{K-K} *and* N_{K-pi} are the 2-BM normalization values which are employed in the calculation of the beam-background. For KK (Kpi), $\overline{CkTRS \cdot CkTAIL \cdot BWTRS}$ ($\overline{CpiTRS \cdot CpiTAIL \cdot BWTRS}$) is applied

5.2.1 2-beam results

5.2.2 KK-beam background

$$N_{KK} = 3 \times \frac{A_{PV_{noAD}}}{A_{PV_{pnn1}}} \times \frac{(\frac{n_{KK}}{r_{KK}})}{R_{KK} - 1} \tag{13}$$

$$\begin{aligned} N_{KK_{loose}} &= 3 \times \frac{0.673}{0.925} \times \frac{(\frac{8}{51/7.})}{61.9 - 1} \\ &= (39.3 \pm 19.5) \times 10^{-3} \end{aligned} \tag{14}$$

$$\begin{aligned} N_{KK_{tight}} &= 3 \times \frac{0.3752}{0.925} \times \frac{(\frac{1}{22/3.})}{59.9 - 1} \\ &= (2.82 \pm 2.82) \times 10^{-3} \end{aligned} \tag{15}$$

5.2.3 $K\pi$-beam background

- Only measure the background in the data before the $\pi\nu\nu(2)$ C_π trigger change. This entails scaling by 2.54 to extrapolate to the full running period.
- Scale by the acceptance for the PV_{pnn1} cut.
- Do not apply ADPV due to lack of statistics (lower statistics compared to KK due to C_π trigger change.

$$N_{K\pi} = 3 \times 2.54 \times \frac{A_{PV_{pnn2}}}{A_{PV_{pnn1}}} \times \frac{(\frac{n_{K\pi}}{r_{K\pi}})}{R_{K\pi} - 1} \tag{16}$$

$$\begin{aligned} N_{K\pi_{loose}} &= 3 \times 2.54 \times \frac{0.639}{0.925} \times \frac{(\frac{10}{84/4.})}{352.5 - 1} \\ &= (7.73 \pm 7.73) \times 10^{-3} \end{aligned} \tag{17}$$

$$\begin{aligned} N_{K\pi_{tight}} &= 3 \times 2.54 \times \frac{0.356}{0.925} \times \frac{(\frac{3}{45/1.})}{274.3 - 1} \\ &= (0.715 \pm 0.715) \times 10^{-3} \end{aligned} \tag{18}$$

5.3 Beam Background Summary

$(\times 10^{-3})$	k034	e787	1/3 loose	1/3 tight	2/3 loose
1-BM	3.86 ± 2.36	1.66 ± 1.66	1.57 ± 1.57	0.35 ± 0.35	3.86 ± 3.86
2-BM KK	0.983 ± 0.983	145.9 ± 145.9	39.3 ± 19.5	2.82 ± 2.82	$71.8\pm$
2-BM Kpi	0.106 ± 0.106	19.7 ± 19.7	7.73 ± 7.73	0.715 ± 0.715	4.61 ± 4.61
2-BM	1.14 ± 1.14	165.6 ± 165.6	43.8 ± 31.7	31.7 ± 31.7	$76.4\pm$
$Total\ Beam$	5.00 ± 2.62	167.3 ± 167.3	45.37 ± 20.08	3.72 ± 3.22	$78.0\pm$

Table 23: **Total Beam-Background.** Scaled to the 3/3 sample. k034 column is the result of e949-pnn1 analysis [6]. e787 is the result of the e787-PNN2 analysis [7]. The other columns are current results that are expanded upon throughout the rest of the tables. The errors are statistical. KB_{live} for k034 is 1.77×10^{12} and for e787 is 1.71×10^{12} . e787 background has been scaled up accordingly for comparison purposes.

6 Muon Background

The muon background is expected to come mainly from $K^+ \to \mu^+\nu\gamma$ and $K^+ \to \pi^0\mu^+\nu$ decays ($K_{\mu 2\gamma}$) in the PNN2 kinematic region. This background is expected to be small, because for these processes to be confused with signal, both the muon has to be misidentified as a π^+ and the photon(s) have to be missed. The cuts used to suppress the muon background are the $\pi^+ \to \mu^+ \to e^+$ decay sequence cuts (TDCUT02) and the pion-muon kinematic separation cut, RNGMOM.

Cuts	1/3 Loose	2/3 Loose
badrun	12892493 (0.00)	25768044 (0.00)
Tnono	12823737 (1.01)	25631012 (1.01)
DUPEV	12823737 (1.00)	25631012 (1.00)
rdtrk	12823737 (1.00)	25631012 (1.00)
trktim	12823737 (1.00)	25631012 (1.00)
target	12823737 (1.00)	25631012 (1.00)
stlay	12823737 (1.00)	25631012 (1.00)
utc	12823737 (1.00)	25631012 (1.00)
rdutm	12823737 (1.00)	25631012 (1.00)
badstc	12823737 (1.00)	25631012 (1.00)
pdc	12823737 (1.00)	25631012 (1.00)
bfdedx	11409696 (1.12)	22803548 (1.12)
bwtrs	8868972 (1.29)	17724324 (1.29)
bftrs	8220794 (1.08)	16427904 (1.08)
bfetcon	8135020 (1.01)	16256902 (1.01)
bfccd	8036604 (1.01)	16060975 (1.01)
cpitrs	7688327 (1.05)	15362723 (1.05)
cpitail	7684992 (1.00)	15355998 (1.00)
cktrs	5335463 (1.44)	10660536 (1.44)
cktail	5062839 (1.05)	10118608 (1.05)
tgqualt	4815371 (1.05)	9625818 (1.05)
timcon	4789227 (1.01)	9573254 (1.01)
tgtcon	4683555 (1.02)	9361755 (1.02)
rvtrs	4666832 (1.00)	9328367 (1.00)
upvtrs	4585317 (1.02)	9165183 (1.02)
delco	3976305 (1.15)	7947312 (1.15)
tggeo	2926088 (1.36)	5848653 (1.36)
combops	2926088 (1.00)	5848653 (1.00)
RNGMOM	1209061 (2.42)	2414194 (2.42)
bfekz	1014599 (1.19)	2025353 (1.19)
epitg	844535 (1.20)	1685549 (1.20)
epimaxk	844535 (1.00)	1685549 (1.00)
targf	806399 (1.05)	1610360 (1.05)
tger	804818 (1.00)	1607188 (1.00)
dtgttp	804809 (1.00)	1607170 (1.00)
rtdif	797785 (1.01)	1592799 (1.01)
drp	796019 (1.00)	1589231 (1.00)
tgktim	789942 (1.01)	1577192 (1.01)
eiccon	755694 (1.05)	1508824 (1.05)
ticcon	755690 (1.00)	1508815 (1.00)
tgedge	750037 (1.01)	1497404 (1.01)
tgenr	731229 (1.03)	1459572 (1.03)
pigap	721184 (1.01)	1439511 (1.01)
combotglik	687003 (1.05)	1371135 (1.05)
tgdbf	670474 (1.02)	1338069 (1.02)
tgdbftip	667741 (1.00)	1332645 (1.00)
tgdvxtip	666148 (1.00)	1329452 (1.00)
tgdvxpi	644754 (1.03)	1286459 (1.03)
combotgbf	644754 (1.00)	1286459 (1.00)
phivtx	621056 (1.04)	1239008 (1.04)
opsveto	609426 (1.02)	1216002 (1.02)
timkf	543459 (1.12)	1084486 (1.12)
npitg	543459 (1.00)	1084486 (1.00)
kic	543336 (1.00)	1084243 (1.00)
tgzfool	530074 (1.03)	1057691 (1.03)
layv	530069 (1.00)	1057676 (1.00)
tgpvcut	526096 (1.01)	1049965 (1.01)
ccdpul	235592 (2.23)	470537 (2.23)
epionk	234363 (1.01)	468036 (1.01)
ccdbadtim	233082 (1.01)	465416 (1.01)
ccdfib	233082 (1.00)	465415 (1.00)
verrng	214824 (1.08)	428927 (1.09)
angli	214732 (1.00)	428734 (1.00)
allkfit	212394 (1.01)	424112 (1.01)
tpics	212345 (1.00)	424014 (1.00)

continued on next page

Cuts	1/3 Loose	2/3 Loose
costd	193686 (1.10)	385979 (1.10)
zfrf	167224 (1.16)	333359 (1.16)
zutout	167085 (1.00)	333090 (1.00)
rsdedxmax	120616 (1.39)	240598 (1.38)
rsdedxcl	70050 (1.72)	139105 (1.73)
rslike	67722 (1.03)	134313 (1.04)
rsdedx	67722 (1.00)	134313 (1.00)
utcqual	64701 (1.05)	128191 (1.05)
prrf	38737 (1.67)	76657 (1.67)
prrfz	33215 (1.17)	65601 (1.17)
comboprrf	33215 (1.00)	65601 (1.00)
tggeo	33215 (1.00)	65601 (1.00)
piflg	26295 (1.26)	51902 (1.26)
tgdedx	26062 (1.01)	51437 (1.01)
pvpnnone	**5598** (4.66)	**11039** (4.66)
elveto	2117 (2.64)	4142 (2.67)
tdfool	2090 (1.01)	4104 (1.01)
tdnn	86 (24.30)	166 (24.72)
evfive	86 (1.00)	166 (1.00)
combotd	**86** (1.00)	**166** (1.00)
Total Rej.	65.09 ± 6.97	66.50 ± 5.12

Table 24: Rejection Branch for Muon Background. (not added yet??? Tight has the tight version of PV, DELCO, TD, BOX applied). The numbers represent the number of events remaining after application of the cut designated on a given row. Number in parenthesis is the rejection of the cut.

Cuts	1/3 Loose	2/3 Loose
badrun	12892493 (0.00)	25768044 (0.00)
Tnono	12823737 (1.01)	25631012 (1.01)
DUPEV	12823737 (1.00)	25631012 (1.00)
rdtrk	12823737 (1.00)	25631012 (1.00)
trktim	12823737 (1.00)	25631012 (1.00)
target	12823737 (1.00)	25631012 (1.00)
stlay	12823737 (1.00)	25631012 (1.00)
utc	12823737 (1.00)	25631012 (1.00)
rdutm	12823737 (1.00)	25631012 (1.00)
badstc	12823737 (1.00)	25631012 (1.00)
pdc	12823737 (1.00)	25631012 (1.00)
bfdedx	11409696 (1.12)	22803548 (1.12)
bwtrs	8868972 (1.29)	17724324 (1.29)
bftrs	8220794 (1.08)	16427904 (1.08)
bfetcon	8135020 (1.01)	16256902 (1.01)
bfccd	8036604 (1.01)	16060975 (1.01)
cpitrs	7688327 (1.05)	15362723 (1.05)
cpitail	7684992 (1.00)	15355998 (1.00)
cktrs	5335463 (1.44)	10660536 (1.44)
cktail	5062839 (1.05)	10118608 (1.05)
tgqualt	4815371 (1.05)	9625818 (1.05)
timcon	4789227 (1.01)	9573254 (1.01)
tgtcon	4683555 (1.02)	9361755 (1.02)
rvtrs	4666832 (1.00)	9328367 (1.00)
upvtrs	4585317 (1.02)	9165183 (1.02)
delco	3976305 (1.15)	7947312 (1.15)
tggeo	2926088 (1.36)	5848653 (1.36)
combops	2926088 (1.00)	5848653 (1.00)
$\overline{TD_{loose}}$	2115217 (1.38)	4226709 (1.38)
box	64304 (32.89)	128749 (32.83)
bfekz	51345 (1.25)	103503 (1.24)
epitg	42559 (1.21)	86159 (1.20)
epimaxk	42559 (1.00)	86159 (1.00)
targf	39886 (1.07)	80451 (1.07)
tger	39838 (1.00)	80308 (1.00)
dtgttp	39836 (1.00)	80308 (1.00)
rtdif	39505 (1.01)	79653 (1.01)
drp	39196 (1.01)	79051 (1.01)
tgktim	38772 (1.01)	78223 (1.01)
eiccon	37943 (1.02)	76624 (1.02)
ticcon	37943 (1.00)	76624 (1.00)
tgedge	37532 (1.01)	75741 (1.01)
tgenr	36831 (1.02)	74276 (1.02)
pigap	36487 (1.01)	73624 (1.01)
combotglik	33959 (1.07)	68304 (1.08)
tgdbf	33040 (1.03)	66489 (1.03)
tgdbftip	32650 (1.01)	65664 (1.01)
tgdvxtip	32455 (1.01)	65316 (1.01)
tgdvxpi	32001 (1.01)	64341 (1.02)

continued on next page

Cuts	1/3 Loose	2/3 Loose
combotgbf	32001 (1.00)	64341 (1.00)
phivtx	29934 (1.07)	60077 (1.07)
opsveto	28194 (1.06)	56624 (1.06)
timkf	24895 (1.13)	50209 (1.13)
npitg	24895 (1.00)	50209 (1.00)
kic	24889 (1.00)	50199 (1.00)
tgzfool	24447 (1.02)	49365 (1.02)
layv	24447 (1.00)	49365 (1.00)
tgpvcut	23721 (1.03)	47882 (1.03)
rngmom	1728 (13.73)	3513 (13.63)
costd	1667 (1.04)	3375 (1.04)
zfrf	1665 (1.00)	3363 (1.00)
zutout	1656 (1.01)	3333 (1.01)
rsdedxmax	1463 (1.13)	2930 (1.14)
rsdedxcl	1303 (1.12)	2627 (1.12)
rslike	1303 (1.00)	2627 (1.00)
rsdedx	1303 (1.00)	2627 (1.00)
utcqual	1173 (1.11)	2410 (1.09)
prrf	1160 (1.01)	2378 (1.01)
prrfz	1063 (1.09)	2184 (1.09)
comboprrf	1063 (1.00)	2184 (1.00)
tggeo	1063 (1.00)	2184 (1.00)
piflg	1028 (1.03)	2114 (1.03)
tgdedx	1006 (1.02)	2062 (1.03)
ccdpul	187 (5.38)	364 (5.66)
epionk	185 (1.01)	362 (1.01)
ccdbadtim	179 (1.03)	353 (1.03)
ccdfib	179 (1.00)	353 (1.00)
verrng	134 (1.34)	258 (1.37)
angli	134 (1.00)	257 (1.00)
allkfit	130 (1.03)	249 (1.03)
tpics	130 (1.00)	249 (1.00)
tgdedx	130 (1.00)	249 (1.00)
chifss	105 (1.24)	210 (1.19)
chifmax	105 (1.00)	210 (1.00)
PV_{pnn2}	**0** (105.00)	**1** (210.00)

Table 25: Normalization Branch for Muon Background. (not added yet??? Tight has the tight version of PV, DELCO, BOX applied). The numbers represent the number of events remaining after application of the cut designated on a given row. Number in parenthesis is the rejection of the cut.

After some setup cuts that remove $K_{\pi 2}$ decays and beam backgrounds, in the normalization branch (Table 25) the loose TDCUT02 is inverted for both the loose and tight regions; this is done to prevent us from looking in the box. When the remaining cuts are applied (KCUTS and PVPNN2), zero events remains in the normalization branch, as shown in Table 25, therefore N=1 will be used for the background estimation. In the rejection branch, RNGMOM is inverted and the rejection of the TDCUT02 is measured on this sample. Using these values, the muon background is

$$N_{muon_{\frac{1}{3}loose}} = 3 \times \frac{N_{loose}}{R_{TD_{loose}} - 1} \tag{19}$$

$$= 3 \times \frac{1 \pm 1}{(65.09 \pm 6.97) - 1}$$

$$= 0.0468 \pm 0.0468 \tag{20}$$

$$N_{muon_{\frac{2}{3}loose}} = \frac{3}{2} \times \frac{N_{loose}}{R_{TD_{loose}} - 1} \tag{21}$$

$$= \frac{3}{2} \times \frac{1 \pm 1}{(66.50 \pm 5.12) - 1}$$

$$= 0.0229 \pm 0.0229 \tag{22}$$

$$N^{scale}_{muon_{tight}} = \frac{A_{PV_{tight}}}{A_{PV_{loose}}} \times \frac{A_{BOX_{tight}}}{A_{BOX_{loose}}} \times \frac{A_{BOX_{tight}}}{A_{BOX_{loose}}} \times N_{muon_{loose}} \quad (23)$$

$$= \frac{0.356}{0.639} \times \frac{0.704}{0.942} \times (0.68) \times \frac{0.704}{0.857} \times 0.0229 \pm 0.0229$$

$$= 0.0053 \pm 0.0053 \quad (24)$$

7 Charge exchange background

The pass2 cuts history is tabulated in Tab. 26 along with the result from 1/3 sample. The result are consistent within statistical uncertainty. With the following formula:

$$N_{CEX} = N_{norm,\ data} \times \frac{N_{targf,\ UMC}}{N_{kpigap,\ UMC}} \times ACC_{unapplied}\ , \quad (25)$$

The background numbers are estimated and summarized in Tab. 27. $ACC_{unapplied}$ is 70% where the contribution of CCDBADFIT was missed in 1/3 note.

8 K_{e4} background

K_{e4} background is estimated with 2/3 sample. The normalization branching of 2/3 sample as well as that from 1/3 sample where the bug of multiplexing is cleared are tabulated in Tab. 28. The background number is summarized in Tab. 29.

9 Background Contamination Studies

This study was initially prompted by Toshio asking how much additional muon contamination was introduced into the $K_{\pi 2}$ target-scatter normalization and rejection branches due to using a set of TD cuts that are looser than the E949 PNN1 ones.

As discussed in [1], three of the ten events remaining at the end of the loose $K_{\pi 2}$ target-scatter rejection branch were classified as being non $K_{\pi 2}$ target-scatter. One of these events was 2-beam, one was K_{e4} and one was likely K_{e4}.

Quantification of the contamination of the $K_{\pi 2}$ target-scatter branches by these three background processes (K_{e4}, muon and 2-beam) would allow corrections to be made to the $K_{\pi 2}$ target-scatter background to remove the double counting of these backgrounds. Generally, the effect of these contaminations will be to cause the backgrounds to be overestimated.

The general method of estimating a background is to identify two sets of uncorrelated cuts (CUT1 and CUT2, collectively known as bifurcation cuts) which provide a large rejection for the background in question. The normalization branch is a sample created by inverting one of these sets of bifurcation cuts (CUT1) to create a sample rich in the background being studied and applying the rest of the cuts to purify the sample. The number of events left after all cuts have been applied in the normalization branch is known

	Tight cuts 1/3	Loose cuts 1/3	Tight cuts 2/3	Loose cuts 2/3
skim123,567	12621399	12621399	25768044	25768044
delco2	7716700	7716700	15743575	15743575
KCUTS	206709	289592	423053	592084
CKTRS	182952(0.885)	256241(0.884)	374726(0.885)	524435(0.885)
CKTAIL	178646(0.976)	250182(0.976)	366054(0.976)	512270(0.976)
CPITRS	126363(0.707)	186280(0.744)	259740(0.709)	382042(0.745)
CPITAIL	126224(0.998)	186108(0.999)	259442(0.998)	381643(0.998)
BWTRS	119382(0.945)	176467(0.948)	245502(0.946)	362127(0.948)
B4DEDX	118158(0.989)	174641(0.989)	242944(0.989)	358323(0.989)
B4TRS	108812(0.920)	161046(0.922)	224029(0.922)	330320(0.921)
B4CCD	107089(0.984)	158536(0.984)	220373(0.983)	325020(0.983)
TIMCON	106186(0.991)	156924(0.989)	218457(0.991)	321662(0.989)
IPIFLG	105642(0.994)	156112(0.994)	217349(0.994)	320044(0.994)
ELVETO	98219(0.929)	145296(0.930)	202144(0.930)	298045(0.931)
TDFOOL	98051(0.998)	145025(0.998)	201803(0.998)	297521(0.998)
TDVARNN	67226(0.685)	133473(0.920)	137530(0.681)	273819(0.920)
PVCUT	188(0.002)	1395(0.010)	426(0.003)	2938(0.010)
KPIGAP	12(0.063)	62(0.044)	15(0.035)	98(0.033)
TGZFOOL	8(0.666)	50(0.806)	13(0.866)	79(0.806)
EPITG	3(0.375)	29(0.580)	5(0.384)	55(0.696)
EPIMAXK	3(1.000)	29(1.000)	5(1.000)	55(1.000)
EPIONK	3(1.000)	29(1.000)	5(1.000)	55(1.000)
TIMKF	2(0.666)	18(0.620)	3(0.600)	39(0.709)
KIC	2(1.000)	14(0.777)	2(0.666)	30(0.769)
TGQUALT	2(1.000)	14(1.000)	2(1.000)	30(1.000)
NPITG	2(1.000)	14(1.000)	2(1.000)	30(1.000)
TGER	2(1.000)	14(1.000)	2(1.000)	29(0.966)
DTGTTP	2(1.000)	14(1.000)	2(1.000)	29(1.000)
RTDIF	2(1.000)	14(1.000)	2(1.000)	29(1.000)
DRP	2(1.000)	14(1.000)	2(1.000)	29(1.000)
TGKTIM	2(1.000)	14(1.000)	2(1.000)	28(0.965)
TGEDGE	2(1.000)	13(0.928)	2(1.000)	27(0.964)
TGDEDX	2(1.000)	13(1.000)	2(1.000)	25(0.925)
TGENR	2(1.000)	13(1.000)	2(1.000)	23(0.920)
PIGAP	2(1.000)	13(1.000)	2(1.000)	22(0.956)
TGLIKE	2(1.000)	9(0.692)	2(1.000)	16(0.727)
TGB4	2(1.000)	5(0.555)	0(0.000)	7(0.437)
PHIVTX	1(0.500)	5(1.000)	0( )	7(1.000)
TPICS	1(1.000)	5(1.000)	0( )	7(1.000)
TGTCON	1(1.000)	5(1.000)	0( )	7(1.000)
B4ETCON	1(1.000)	5(1.000)	0( )	7(1.000)
TGGEO	1(1.000)	3(0.600)	0( )	0(0.000)

Table 26: The pass2 cuts history of the normalization branch of the 1/3 and 2/3 data for the CEX study.

	Tight cuts 1/3	Loose cuts 1/3	Tight cuts 2/3	Loose cuts 2/3
N_{norm}	1	3	1	1
$N_{targf,\ UMC}$	6^{+6}_{-2}	50^{+33}_{-10}	6^{+6}_{-2}	50^{+33}_{-10}
$N_{kpigap,\ UMC}$	3332	4136	3332	4136
N_{CEX}	$0.0038 \pm 0.0038^{+0.0038}_{-0.0013}$	$0.076 \pm 0.044^{+0.058}_{-0.015}$	$0.0019 \pm 0.0019^{+0.0019}_{-0.0006}$	$0.013 \pm 0.013^{+0.001}_{-0.003}$

Table 27: CEX background number normalized to 3/3 data. The first error of N_{CEX} is statistical and the second error is the estimated systematic uncertainty due to TGPV, OPSVETO and CCDPUL.

as the normalization N. The rejection branch is created by inverting the second set of bifurcation cuts (CUT2) to create another sample rich in the studied background with which to measure the rejection R of the set of cuts inverted to created the normalization branch. The background bg is estimated by the equation

$$bg = \frac{N}{R-1}.$$

Contamination from another background process will usually inflate the value estimated by this method. The normalization N will contain contamination events in addition to the background events. The rejection of the bifurcation cuts on the contamination events will generally be significantly lower than on the background being measured. The contamination events in the rejection branch will usually result in a measured rejection R that is lower than the rejection would be for an uncontaminated sample.

The typical effect of the contamination in both the normalization N and the rejection R values is that they inflate the background estimate in question. Since background estimates are made for each of the contamination processes, this contamination ends up inflating the total background estimate by double counting the contribution of the contamination processes. This inflated total background estimate reduces the central value of the branching fraction calculated from this analysis.

Note that the contamination estimates in this section were measured only on the 1/3 data sample and before the the 2 sets of corrections to the multiplexing of low-gain CCD fibers (see Sections 2.5 and 2.6). Since the findings of the contamination study were that the levels of contamination are negligible and the fixes to the multiplexing of low-gain CCD fibers had less than a 1% effect on CCDPUL performance, the measurements were not redone to account for the fixes to the multiplexing of low-gain CCD fibers.

It was not possible to use data to make an estimate of K_{e4} contamination in the $K_{\pi 2}$ target-scatter background evaluation. This was due to the lack of cuts that specifically target K_{e4} with a large rejection as compared to the cut's rejection of $K_{\pi 2}$ target-scatter.

9.1 Muon Contamination in the $K_{\pi 2}$ Target-Scatter Background

The bifurcation cuts used to estimate the muon background are (CUT1) the collection of cuts known as TDCUT02 and (CUT2) RNGMOM.

	Tight cuts 1/3	Loose cuts 2/3	Tight cuts 2/3	Loose cuts 2/3
skim123,456	12892493	12892493	25768044	25768044
KCUTS	565304	764574	1131416	1530745
PCUTS	120637	179885	242199	360123
TDCUTS	76142	152880	152260	306179
PVCUT	516	3011	1020	6048
DELC	268(0.519)	1648(0.547)	554(0.543)	3350(0.553)
DELC3	235(0.876)	1644(0.997)	481(0.868)	3340(0.997)
TGZFOOL	224(0.953)	1579(0.960)	463(0.962)	3215(0.962)
R-cut	222(0.991)	1554(0.984)	446(0.963)	3142(0.977)
PVICVC	138(0.621)	1118(0.719)	311(0.697)	2343(0.745)
B4EKZ	118(0.855)	933(0.834)	254(0.816)	1853(0.790)
EPITG	78(0.661)	569(0.609)	131(0.515)	1080(0.582)
EPIMAXK	78(1.000)	569(1.000)	131(1.000)	1080(1.000)
TIMKF	59(0.756)	422(0.741)	103(0.786)	816(0.755)
KIC	58(0.983)	410(0.971)	102(0.990)	804(0.985)
TGQUALT	56(0.965)	374(0.912)	94(0.921)	714(0.888)
NPITG	56(1.000)	374(1.000)	94(1.000)	714(1.000)
TGER	56(1.000)	374(1.000)	94(1.000)	712(0.997)
TARGF	53(0.946)	359(0.959)	85(0.904)	669(0.939)
DTGTTP	53(1.000)	359(1.000)	85(1.000)	669(1.000)
RTDIF	53(1.000)	356(0.991)	85(1.000)	661(0.988)
DRP	47(0.886)	327(0.918)	80(0.941)	598(0.904)
TGKTIM	47(1.000)	327(1.000)	80(1.000)	592(0.989)
TGEDGE	45(0.957)	312(0.954)	79(0.987)	558(0.942)
TGDEDX	41(0.911)	287(0.919)	64(0.810)	506(0.906)
TGENR	40(0.975)	282(0.982)	63(0.984)	499(0.986)
PIGAP	38(0.950)	277(0.982)	62(0.984)	491(0.983)
TGLIKE	34(0.894)	257(0.927)	57(0.919)	446(0.908)
TGB4	34(1.000)	250(0.972)	55(0.964)	433(0.970)
PHIVTX	14(0.411)	105(0.420)	25(0.454)	187(0.431)
CHI567	13(0.928)	93(0.885)	15(0.600)	155(0.828)
CHI5MAX	13(1.000)	93(1.000)	15(1.000)	155(1.000)
VERRNG	10(0.769)	81(0.870)	14(0.933)	137(0.883)
ANGLI	10(1.000)	81(1.000)	14(1.000)	137(1.000)
TGFITALLK	10(1.000)	80(0.987)	14(1.000)	130(0.948)
TPICS	10(1.000)	80(1.000)	14(1.000)	130(1.000)
TGTCON	10(1.000)	80(1.000)	14(1.000)	130(1.000)
B4ETCON	10(1.000)	80(1.000)	14(1.000)	129(0.992)
CCDBADTIM	9(0.900)	76(0.950)	13(0.928)	124(0.961)
CCDBADFIT	6(0.666)	66(0.868)	13(1.000)	111(0.895)
CCD31FIB	6(1.000)	66(1.000)	13(1.000)	111(1.000)
CCDPUL	1(0.166)	4(0.060)	0(0.000)	7(0.063)
EPIONK	1(1.000)	4(1.000)	0( )	7(1.000)

Table 28: The pass2 cuts history of the normalization branch of the 2/3 data for K_{e4} study. R-cut is $\overline{\text{TGPV} \cdot \text{OPSVETO}}$.

	Tight cuts 1/3	Loose cuts 1/3	Tight cuts 2/3	Loose cuts 2/3
N_{norm}	1	4	1	7
$R_{TGPV\cdot OPSVETO}$	88^{+263}_{-70}	52^{+121}_{-29}	88^{+263}_{-70}	52^{+121}_{-29}
$N_{K_{e4}}$	$0.034 \pm 0.017^{+0.071}_{-0.013}$	$0.235 \pm 0.059^{+0.155}_{-0.083}$	$0.017 \pm 0.017^{+0.071}_{-0.013}$	$0.206 \pm 0.078^{+0.271}_{-0.145}$

Table 29: K_{e4} background number normalized to 3/3 data. The first error of $N_{K_{e4}}$ is statistical and the second error is from $R_{TGPV\cdot OPSVETO}$.

9.1.1 Acceptance and Rejection of the Muon Bifurcation Cuts

The rejection of RNGMOM ($R_{\rm RNGMOM}$) for muon events was measured in the muon background normalization branch (see [1]) by inverting TDCUT02. The rejection of TDCUT02 ($R_{\rm TDCUT02}$) for muon events was measured in the muon background rejection branch of the same technote by inverting RNGMOM. The combined rejection of these cuts R_μ can be calculated

$$\begin{aligned} R_\mu &= R_{\rm RNGMOM} \times R_{\rm TDCUT02} \\ &= (14.09 \pm 0.43) \times (107.82 \pm 32.36) \\ &= 1510 \pm 458 \end{aligned} \tag{26}$$

The acceptance of these cuts for pion events was measured directly using a modified version of the rejection branch for the $K_{\pi 2}$ target-scatter background estimate. The modifications are that TDCUT02 and RNGMOM were removed from the setup cuts and the kinematic box was changed from the PNN2 loose kinematic box to the $K_{\pi 2}$-peak kinematic box. The setup cuts are shown in Table 30.

Setup cuts for measuring acceptance of RNGMOM and TDCUT
SKIM5, STLAY, VALID_TRIG, HEX_AFTER
PSCUT06
DELCO3
KINCUT06 (without RNGMOM)
KP2-PEAK KINEMATIC BOX

Table 30: [Setup cuts for measuring acceptance of RNGMOM and TDCUT] The setup cuts for measuring acceptance of RNGMOM and TDCUT.

After the setup cuts have been applied, the 13 classes described in Table 3 are applied and the performance of the cuts RNGMOM and TDCUT02 are measured before and after application of the photon veto as shown in Table 31. For each of the classes the measured acceptance of these muon bifurcation cuts is equal before and after the application of the photon veto cut within statistical error. The extracted acceptance A_π can be taken as the average of the highest and lowest acceptances (ignoring CLASS11 due to much mower

statistics) measured before the application of the photon veto with the difference between these extreme values setting the bounds for the error:

$$A_\pi = 0.8813 \pm 0.0035. \tag{27}$$

Acceptances of RNGMOM×TDCUT02 for $K_{\pi 2}$-peak events

CLASS	BEFORE PV	AFTER PV60
1	$60670/68875 = 0.8809 \pm 0.0012$	$35/41 = 0.8537 \pm 0.0552$
2	$147602/167612 = 0.8806 \pm 0.0008$	$121/140 = 0.8643 \pm 0.0289$
3	$59426/67403 = 0.8817 \pm 0.0012$	$54/61 = 0.8852 \pm 0.0408$
4	$61702/69988 = 0.8816 \pm 0.0012$	$38/49 = 0.7755 \pm 0.0596$
5	$183123/207913 = 0.8808 \pm 0.0007$	$147/171 = 0.8596 \pm 0.0266$
6	$86699/98303 = 0.8820 \pm 0.0010$	$72/82 = 0.8780 \pm 0.0361$
7	$89456/101469 = 0.8816 \pm 0.0010$	$57/68 = 0.8382 \pm 0.0447$
8	$13635/15412 = 0.8847 \pm 0.0026$	$11/14 = 0.7857 \pm 0.1097$
9	$172311/195578 = 0.8810 \pm 0.0007$	$141/164 = 0.8598 \pm 0.0271$
10	$29962/34135 = 0.8778 \pm 0.0018$	$28/32 = 0.8750 \pm 0.0585$
11	$3009/3395 = 0.8863 \pm 0.0054$	$2/2 = 1.0000 \pm 0.0000$
12	$159602/181255 = 0.8805 \pm 0.0008$	$129/149 = 0.8658 \pm 0.0279$
13	$65623/74452 = 0.8814 \pm 0.0012$	$58/67 = 0.8657 \pm 0.0417$

Table 31: The acceptance of RNGMOM×TDCUT02 is measured for $K_{\pi 2}$-peak events before and after the application of the photon veto cut at the 60% level (PV60) for each of the 13 classes from the $K_{\pi 2}$ target-scatter rejection branch.

9.1.2 Muon Contamination in the Normalization Branch

To determine the amount of muon contamination in the normalization branch, the number of events N left at the end of the normalization branch is treated as being made up of either muon N_μ or pion N_π events. Written in equation form, this looks like

$$N = N_\pi + N_\mu \tag{28}$$

Since we know the performance of the muon bifurcation cuts (RNGMOM and TDCUT02) with respect to pions (A_π) and muons (R_μ), we can move these cuts to the bottom of the $K_{\pi 2}$ target-scatter normalization branch and measure the number of events n remaining before these cuts are applied. This allows us to write the following equation

$$n = \frac{N_\pi}{A_\pi} + R_\mu N_\mu \tag{29}$$

The amount of muon contamination left at the end of the normalization branch can be represented by the quantity f,

$$f = \frac{\frac{n}{N} - \frac{1}{A_\pi}}{R_\mu - \frac{n}{N}} \tag{30}$$

Taking the values from Section 9.1.1 ($A_\pi = 0.8813 \pm 0.0035$ and $R_\mu = 1510 \pm 458$) and the measured values $N = 510$ and $n = 1054$, we can solve for the value f,

$$f = (6.18 \pm 1.93) \times 10^{-4} \tag{31}$$

Using these conventions, the corrected (uncontaminated) normalization number N', which is the number of pions at the end of the normalization branch can be written as

$$\begin{aligned} N' &= N(1-f) && (32)\\ &= 509.7 \pm 22.6 && (33) \end{aligned}$$

9.1.3 Muon Contamination in the Rejection Branch

The method used to determine the amount of muon contamination in the rejection branch is very similar to that for the normalization branch except the amount of contamination has to be measured before and after the bifurcation cut (CUT1) for which the rejection is being measured. For $K_{\pi 2}$ target-scatter, this cut is the photon veto.

Again, we will call the number of events left at the end of the branch N where each class is its own branch and the end of the branch is considered to be after the photon veto has been applied. The number of events before the photon veto is applied will be denoted M. Using these conventions, the photon veto rejection R_{PV} is given by

$$R_{\mathrm{PV}} = \frac{M}{N} \tag{34}$$

We can examine the amount of muon contamination both before and after the photon veto has been applied by treating M and N as being made up of muon and pion events as with the normalization branch method:

$$\begin{aligned} M &= M_\pi + M_\mu, && (35)\\ N &= N_\pi + N_\mu. && (36) \end{aligned}$$

Again we can use the known performance of the muon bifurcation cuts (RNGMOM and TDCUT02) with respect to pions (A_π) and muons (R_μ) to solve for the fraction of the events which are muon contamination. These muon bifurcation cuts can be applied immediately before the end of the branch (after the photon veto) giving a value n before the muon bifurcation cuts and N after the bifurcation cuts. The same can be done by applying these muon bifurcation cuts immediately before the photon veto is applied giving a value m before the muon bifurcation cuts and M after the bifurcation cuts.

$$\begin{aligned} m &= A_\pi M_\pi + R_\mu M_\mu, && (37)\\ n &= A_\pi N_\pi + R_\mu N_\mu. && (38) \end{aligned}$$

The amount of muon contamination before and after the photon veto are applied can be represented by the quantities f_M and f_N respectively,

$$f_M = \frac{\frac{m}{M} - \frac{1}{A_\pi}}{R_\mu - \frac{m}{M}}, \tag{39}$$

$$f_N = \frac{\frac{n}{N} - \frac{1}{A_\pi}}{R_\mu - \frac{n}{N}}. \tag{40}$$

Using these conventions, the corrected (uncontaminated) photon veto rejection is given by

$$R'_{\rm PV} = \frac{M(1-f_M)}{N(1-f_N)} \quad (41)$$

$$= 2665.9 \pm 843.3 \quad (42)$$

Table 32 shows the values used to arrive at a corrected value for the photon veto rejection.

Quantity	Before PV60	After PV60
Muon bifurcation cuts not applied	$m = 31119$	$n = 38$
Muon bifurcation cuts applied	$M = 26612$	$N = 10$
f-value	$f_M = (2.27 \pm 0.78) \times 10^{-5}$	$f_N = (1.77 \pm 0.87) \times 10^{-3}$
Corrected value	$M' = M(1-f_M)$ $= 26611.4 \pm 163.1$	$N' = N(1-f_N)$ $= 9.98 \pm 3.16$
$R'_{\rm PV} = M'/N'$	2665.9 ± 843.3	
$R_{\rm PV}$ (K073.v1 [1])	2661.3 ± 841.4	

Table 32: This table shows the values used to arrive at a photon veto rejection after the effects of muon contamination have been removed.

9.1.4 Background Estimate Corrected for Muon Contamination

Numbers from the previous two sections can be used to estimate the background without muon contamination.

$$bg' = \frac{3N'}{R'_{\rm PV} - 1} \quad (43)$$

$$= \frac{3(509.6 \pm 22.6)}{(2665.9 \pm 846.6) - 1} \quad (44)$$

$$= 0.574 \pm 0.184 \quad (45)$$

The value from K073.v1 [1] is 0.575 ± 0.184.

Since the central values of these two quantities agree to better than 1%, we can consider the muon contamination in the $K_{\pi 2}$ target-scatter background to be negligible.

9.2 Double-Beam Contamination in the $K_{\pi 2}$ Target-Scatter Background

Due to a lack of acceptance and rejection information for the rejection branch bifurcation cuts for double-beam background, only the normalization branch bifurcation cuts will be used in the study.

The rejection of CKTRS, CKTAIL and BWTRS will be denoted R_{KK} and the rejection of CPITRS, CPITAIL and BWTRS will be denoted R_{KP}. These rejections are taken from the double-beam rejection branch (see Table 31 of [1]). The acceptance of these cuts for pion events was taken from the beam acceptance (Table 46 of [1]) which uses $K_{\mu 2}$ monitors which have had cuts applied to ensure it looks like a single K^+ decay with no photons. These values are summarized in Table 33

	KK Branch	KP Branch
Cuts	CKTRS·CKTAIL·BWTRS	CPITRS·CPITAIL·BWTRS
Acceptance	$A_{KK} = 0.8973 \pm 0.0002$	$A_{KP} = 0.9159 \pm 0.0002$
Rejection	$R_{KK} = 61.9 \pm 9.8$	$R_{KP} = 352.5 \pm 124.5$

Table 33: Acceptances and rejections of double-beam bifurcation cuts

9.2.1 Double-Beam Contamination in the Normalization Branch

The method for determining the double-beam contamination in the $K_{\pi 2}$ target-scatter normalization branch is the same as that described for muon contamination, but with with a different set of cuts for each of the KK and KP double-beam contamination. Since the contamination due to each of these backgrounds is expected to be very small, the KK contamination will be ignored for the KP contamination study and the KP contamination ignored for the KK contamination study.

The following discussion lays out the equations used to determine the amount of KK double-beam contamination, but the same equations all apply for the KP double-beam contamination with the KP notation replacing the KK notation. To determine the amount of KK contamination in the normalization branch, the number of events N left at the end of the normalization branch is treated as being made up of either $K_{\pi 2}$ target-scatter N_π or KK double-beam N_{KK} events. Written in equation form, this looks like:

$$N = N_\pi + N_{KK}. \tag{46}$$

Since we know the performance of the KK double-beam rejection branch bifurcation cuts (CKTRS, CKTAIL and BWTRS) with respect to kp2 target-scatter events (A_{KK}) and KK double-beam (R_{KK}), we can move these cuts to the bottom of the kp2 target-scatter normalization branch and measure the number of events n remaining before these cuts are applied. This allows us to write the following equation

$$n = \frac{N_\pi}{A_{KK}} + R_{KK} N_{KK} \tag{47}$$

The amount of muon contamination left at the end of the normalization branch can be represented by the quantity f,

$$f = \frac{\frac{n}{N} - \frac{1}{A_{KK}}}{R_{KK} - \frac{n}{N}} \tag{48}$$

Table 34 shows the values used to determine the fractional contamination for KK and KP double-beam in the normalization branch.

	KK Branch	KP Branch
n	522	502
N	482	472
f-value	$f_{KK} = -0.00051 \pm 0.00024$	$f_{KP} = -0.00084 \pm 0.00020$
Corrected normalization $N' = N(1-f)$	$N'_{KK} = 510.3 \pm 22.6$	$N'_{KP} = 510.4 \pm 22.6$

Table 34: Correcting for double-beam contamination in the $K_{\pi 2}$ normalization branch.

9.2.2 Double-Beam Contamination in the Rejection Branch

The method for determining the double-beam contamination in the kp2 target scatter rejection branch is also similar to that described for muon contamination with the bifurcation cuts from the KK or KPi double-beam contamination instead of the muon bifurcation cuts. Again contamination due to one type of double-beam process (KK or KPi) can be ignored when studying the other.

The following discussion lays out the equations used to determine the amount of KK double-beam contamination, but the same equations all apply for the KPi double-beam contamination with the KPi notation replacing the KK notation. As with the muon contamination in the rejection branch, the amount of contamination has to be measured before and after the photon veto is applied at then end of the rejection branch.

The definitions for M and N can be found in Section 9.1.3. We can examine the amount of KK double-beam contamination both before and after the photon veto has been applied by treating M and N as being made up of muon and pion events as with the normalization branch method:

$$M = M_\pi + M_{KK}, \tag{49}$$
$$N = N_\pi + N_{KK}. \tag{50}$$

These KK double-beam bifurcation cuts can be applied immediately before the end of the branch (after the photon veto) giving a value n before the KK double-beam bifurcation cuts and N after the bifurcation cuts. The same can be done by applying these KK double-beam bifurcation cuts immediately before the photon veto is applied giving a value m before the KK double-beam bifurcation cuts and M after the bifurcation cuts.

$$m = A_{KK}M_\pi + R_{KK}M_{KK}, \tag{51}$$
$$n = A_{KK}N_\pi + R_{KK}N_{KK}. \tag{52}$$

The amount of KK double-beam contamination before and after the photon veto are applied can be represented by the quantities f_M and f_N respectively, as defined in Section 9.1.3. Tables 35 and 36 show the values used to arrive at values for the photon veto rejection after being corrected for each of the double-beam processes.

Quantity	Before PV60	After PV60
Double-beam bifurcation cuts not applied	$m = 26850$	$n = 12$
Double-beam bifurcation cuts applied	$M = 25291$	$N = 9$
f-value	$f_M = (-4.82 \pm 1.50) \times 10^{-5}$	$f_N = (13.1 \pm 15.2) \times 10^{-5}$
Corrected value	$M' = M(1 - f_M)$ $= 26614.3 \pm 163.1$	$N' = N(1 - f_N)$ $= 9.99 \pm 3.16$
$R'_{\rm PV}(KK) = M'/N'$	2661.7 ± 841.9	

Table 35: The KK Double-Beam Contamination in Photon Veto Rejection in the $K_{\pi 2}$ target-scatter rejection branch. This table shows the values used to arrive at a photon veto rejection after the effects of KK double-beam contamination have been removed.

Quantity	Before PV60	After PV60
Double-beam bifurcation cuts not applied	$m = 26200$	$n = 9$
Double-beam bifurcation cuts applied	$M = 25291$	$N = 9$
f-value	$f_M = (-6.54 \pm 2.01) \times 10^{-5}$	$f_N = (-8.93 \pm 2.73) \times 10^{-5}$
Corrected value	$M' = M(1 - f_M)$ $= 26614.7 \pm 163.1$	$N' = N(1 - f_N)$ $= 10.00 \pm 3.16$
$R'_{\rm PV}(KPi) = M'/N'$	2661.2 ± 841.8	

Table 36: The KP Double-Beam Contamination in Photon Veto Rejection in the $K_{\pi 2}$ target-scatter rejection branch. This table shows the values used to arrive at a photon veto rejection after the effects of KP double-beam contamination have been removed.

9.2.3 Background Estimates Corrected for Double-Beam Contamination

Numbers from the previous two sections can be used to estimate the background after being corrected for each of the double-beam processes.

$$bg'_{KK} = \frac{3N'}{R'_{\rm PV} - 1} \tag{53}$$

$$= \frac{3(510.3 \pm 22.6)}{(2661.7 \pm 841.8) - 1} \tag{54}$$

$$= 0.575 \pm 0.184 \tag{55}$$

$$bg'_{KP} = \frac{3N'}{R'_{\rm PV} - 1} \quad (56)$$

$$= \frac{3(510.4 \pm 22.6)}{(2661.2 \pm 841.8) - 1} \quad (57)$$

$$= 0.576 \pm 0.184 \quad (58)$$

Since the central values of these two quantities agree to better than 1% with the value from K073.v1 [1] of 0.575 ± 0.184 we can consider both of the double-beam contaminations in the $K_{\pi 2}$ target-scatter background to be negligible.

10 Acceptance

Needs to be updated for 2/3 analysis.

11 Kaon exposure

As described in the 1/3 analysis note [1], The total KB_{Live} was measured to be 1.7096×10^{12}.

12 Single Cut Failure Study

12.1 Comparison of Skim and tape ntuple productions

The 1/3 Skim (Tape) production in Table 37 is using the pnn2_07 (pnn2) data set which was created with the latest executable on the skimmed data on disk (on tape). It would appear that we have 29 events which differ between the two data sets. However, the number of events are 31.

There are 31 events which are observed in the final production (tape), but are not observed in the 'skim' production. 30 of these events were not seen in the 1-cut study, since the ntuples containing these events were missing. The ntuples were possibility accidently deleted or the PASS2 jobs crashed during production. Event 247077 Run 49038 previously failed the groups: PV(not AD, not TG) and π^+ energy in K^+ fiber.

There are two events which become two-cut failures in the

13 Sensitivity

13.1 Junk method

When the Pnn2 analysis goes to its final stage the features of junk method were studied intensively. It inherited some nice similar behavior from the one cell Bayesian theorem. Problems with multi cells case seems get an easy approximate solution. However some

Group	1/3 Skim production	1/3 Tape production
BOX	36 (0)	41 (0)
PV(no AD, no TG)	190 (20)	214 (22)
ADPV	0	0
DELC3	0	0
B4EKZ	0	0
TGZFOOL	0	0
Extra TG Energy	1 (0)	1 (0)
π^+ energy in K^+ fiber	3 (2)	3 (2)
TG/IC	1 (1)	1 (1)
TD	0	0
Kinematics	2 (1)	2 (1)
Beam	0	0
Other	3 (1)	3 (1)
Total	236 (25)	265 (27)

Table 37: Number of single-cut failures listed by grouped-cuts. "true" single-cut failures are listed in parenthesis and refer to events which only fail one individual cut within the cut group.

hidden issues have to pop up when too many expectation is given to it. Past pnn results were published with junk method. It is not recommended to switch to another approach. But people should have better understanding of the result.

13.1.1 Bayesian theorem

Basic

$$\begin{aligned} P(s|n) &= \frac{P(n|s)P(s)}{P(n)} \\ &= \frac{P(n|s)P(s)}{\int_0^\infty P(n|s)P(s)ds} \end{aligned} \tag{59}$$

- n: number of observed events.
- s: expected signal.
- $P(s)$: prior distribution.
- $P(s|n)$: the probability of s signal with n events observed.

Single channel Assuming a poisson process with signal and background, corresponding to a upper limit N of s the confidence level is:

$$\begin{aligned} 1-\epsilon &= 1 - \frac{e^{-(b+N)}\sum_{n=0}^{n_0}\frac{(b+N)^n}{n!}}{e^{-b}\sum_{n=0}^{n_0}\frac{b^n}{n!}} \\ &= 1 - \frac{\sum_{n=0}^{n_0} P(n|b+N)}{\sum_{n=0}^{n_0} P(n|b)} \\ CL &= 1 - CL_s \\ &= 1 - \frac{CL_{s+b}}{CL_b} \end{aligned} \tag{60}$$

- N: upper limit of signal
- b: background prediction
- n_0: observed events

Here a uniform prior distribution is assumed for $P(s)$ if nothing is known about the signal, like searching for a new phenomena. However it is not the only one choice of that. This presents an analytic, exact solution. In the last two lines of this equations some expression is replaced by some shorthand words, ie. CL, CL_{s+b}, CL_b. CL_{s+b} stands for the poisson probability of observing n event with signal plus background $(b+N)$ assumption. CL_b is the one for background only assumption.

What is CL?

- Given observed events n_0, the probability of $s <= N$ is CL.
- If $s = N$, the probability to find more than n_0 events is CL.

The above two explanations are equivalent. But the form of CL equals the ratio of CL_{s+b} over CL_b is quite accidental. As far as my ability can reach there is no primary physics reason for that.

13.1.2 Junk method (Extended Bayesian limit for multi cells)

- It is based on the last two lines of Equ. 60.
- The CL of this result cannot be understood as a usual probability.
- It can combine the results from multi cells.

- Some reviews tells its ability to distinguish background and signal.

Assume there are many cells, from 1 to m, and each of them have its expected signal s_i and background b_i where i is the index for cells. Then some events ($0 \to \infty$) are observed in some of these cells. To distribute these events into each cell there are lots of combinations. For each of the combination, α is used for the index of combinations and d_i is used to denote the number of observed events in the ith cell then three quantities are defined:

- X_α, test statistic. One choice of that is likelihood ratio.
- $P_\alpha(s+b)$, the probability of the appearance this combination with the assumption of signal and background.
- $P_\alpha(b)$, the probability of the appearance this combination with the assumption of background only.

$$\begin{aligned} X_\alpha &= \prod_{i=1}^{m} \frac{e^{-(b_i+s_i)}\frac{(b_i+s_i)^{d_i}}{d_i!}}{e^{-b_i}\frac{b_i^{d_i}}{d_i!}} \\ &= \prod_{i=1}^{m} e^{-s_i}(1+\frac{s_i}{b_i})^{d_i} \end{aligned} \tag{61}$$

A sequence of combinations can be defined as the ascending order of X_α. Here comes two definitions which are analogs of Equ. 60. "obs" is refer to the real experimental yield.

$$\begin{aligned} P_{s+b}(X_\alpha < X_{obs}) &= \sum_{X_\alpha < X_{obs}} P_\alpha(s+b) \\ P_b(X_\alpha < X_{obs}) &= \sum_{X_\alpha < X_{obs}} P_\alpha(b) \end{aligned} \tag{62}$$

A CL is defined as

$$\begin{aligned} CL &= 1 - CL_s \\ &= 1 - \frac{CL_{s+b}}{CL_b} \end{aligned} \tag{63}$$

Of course it's identical to the single cell case.

13.1.3 BR in junk method

The interesting quantity to be estimated is branching fraction, BR. It is separated from s to make the following discussion more straightforward. SES_i is the single event sensitivity for the ith cell. X_α and CLs will be functions of BR.

$$s_i = SES_i \times BR \tag{64}$$

For pnn analysis the BR which makes X_{obs} reach its maximum is used as the central value of branching fraction. The BR range corresponding to CL_s interval $(50 \pm 34)\%$ is referred to as 68% coverage.

13.1.4 Uncorrelated and correlated uncertainties

Uncorrelated uncertainties of signal and background prediction are treated as a gaussian function in this approach. A gaussian convolution is going to be calculated in junk's code through a numerical integration, see [9]. A global gaussian distribution is generated for every correlated uncertainty. Every correlated variable is changing according that with the same phase, for instance:

$$\begin{aligned} x &\sim Gauss(0,1) \\ SES_1 &= \sigma_1 * x \\ SES_2 &= \sigma_2 * x \\ &... \end{aligned} \tag{65}$$

where x is gaussian variable, σ_i is one standard deviation of SES_i and here SES_1 and SES_2 are 100 percent correlated. In junk's code the negative numbers are truncated. In the following sections the integrations steps are tried to be broken down to get better understanding of that.

13.1.5 An example for one cell

An example of one cell case is given which is of the strict statistic meaning. It is the basic step to understand more complicated multi cells situation.

For one cell:

$$\begin{aligned} X &= e^{-s}(1+\frac{s}{b})^d \\ CL_s &= \frac{\sum_{n=0}^{d} P(n|b+s)}{\sum_{n=0}^{d} P(n|b)} = \frac{e^{-s}\sum_{n=0}^{d} \frac{(b+s)^n}{n!}}{\sum_{n=0}^{d} \frac{b^n}{n!}} \end{aligned} \tag{66}$$

Increase of candidates The first test is done by varying the possible candidate, see Fig. 9. (Assuming SES=0.5, b=0.2, no error for SES and b, and d changing from 0 through 5.) With the increasing of d the central value also increase. As well the 68% coverage position and interval also increases. However the relative error will decrease (error/central value).

Increase of SES This test is done with b=0.2, d=2. The SES is set to 0.2, 0.3 ... 0.8. No error is assumed in this test. See Fig. 10 For two candidates the formulas is quite simple.

$$\begin{aligned} X &= e^{-s}(1+\frac{s}{b})^d \\ CL_s &= \frac{e^{-s}(1+(b+s)+(b+s)^2/2)+...}{1+b+b^2/2+...} \end{aligned} \tag{67}$$

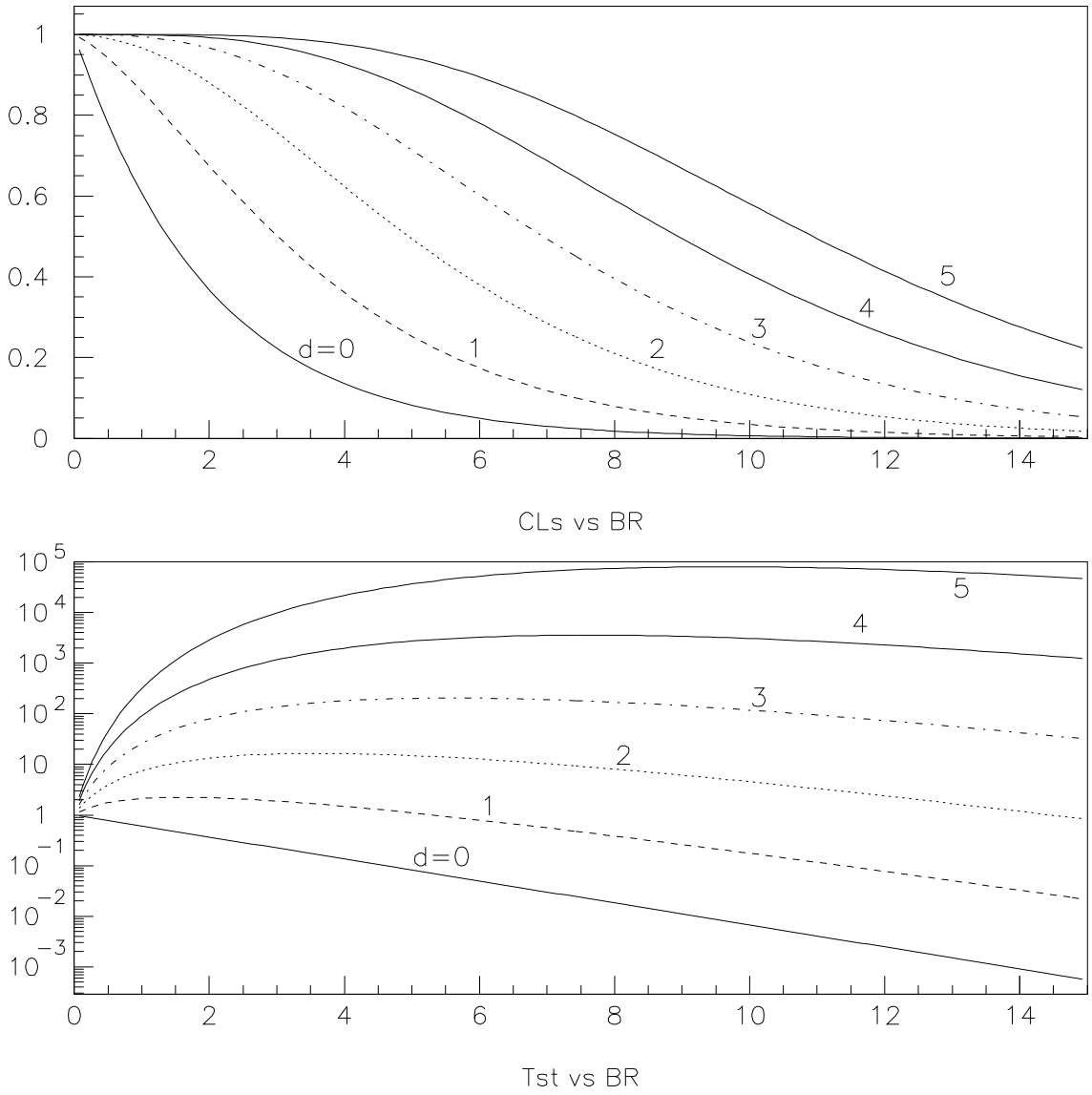

Figure 9: One cell with different number of event observed. The different d is labeled in each curve. The plot on the top is for CL_s, the one on the bottom is for test statistics.

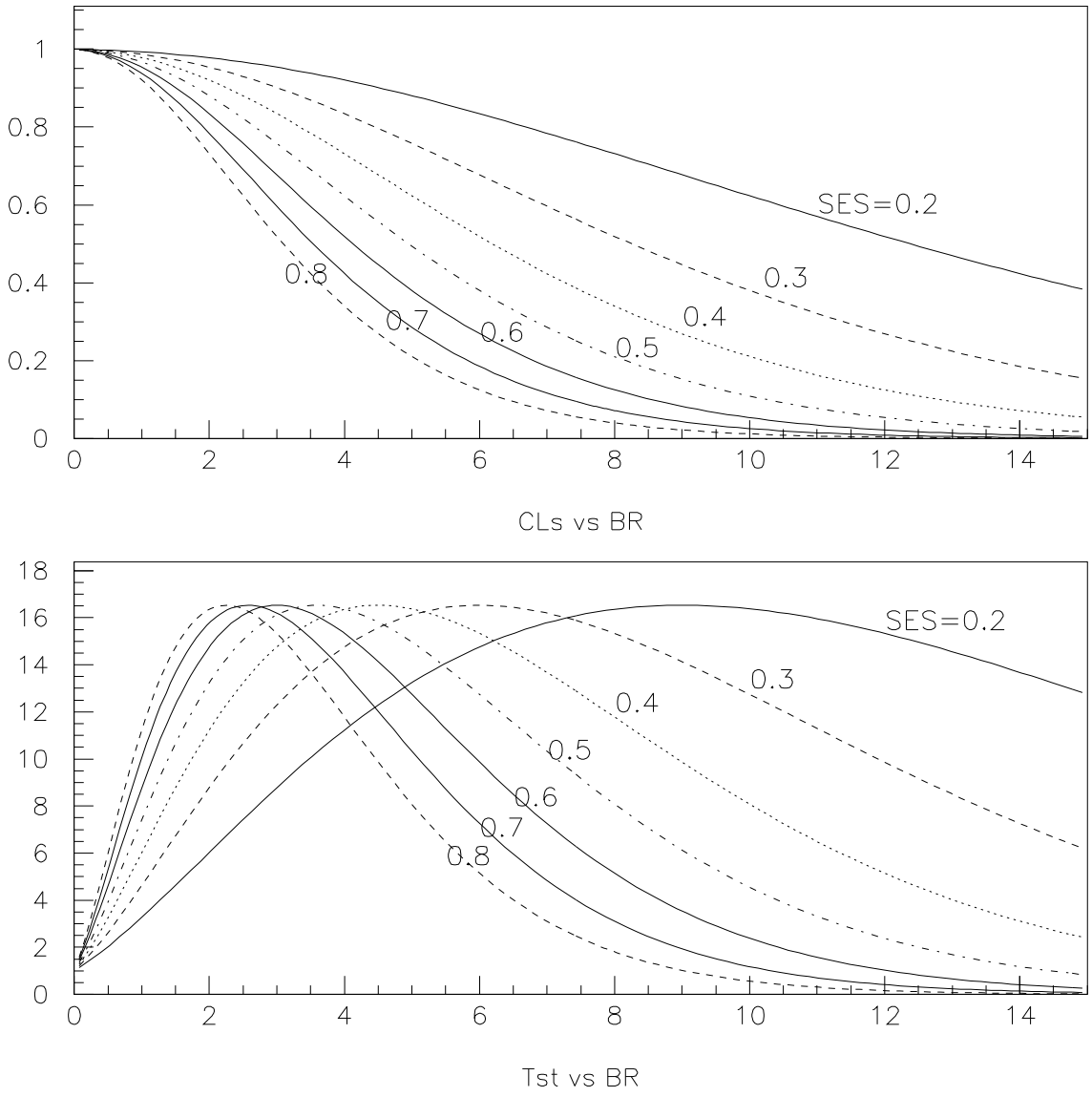

Figure 10: One cell with different SES. The SES for each curve is labeled in the plots. The plot on the top is for CL_s, the one on the bottom is for test statistics.

SES **uncertainty** This is an example very close to reality. Suppose b=0.2 and no error for it. The SES is 0.5 ± 0.1 where 0.1 is one time of deviation. Just image the coarsest approximation for the integration is going to be made. Only take the three point in the gaussian curve, one in the central, the other two ones are at one time of positive deviation and negative deviation respectively. This could be accomplished by taking three curves in Fig. 10, SES=0.4, 0.5 and 0.6 and then get an average of them. So the new test statistics will shifted and the CL_s curve will intersect with the old one (SES=0.5, no error) at some place.

Put this example into code (61 steps for integration approximation), it gives Fig. 11. The 68% interval is larger than that without error as expected.

Increase of background The case of with different background prediction can also be understood by Equ. 67. The understanding of increasing background will help to get a feeling of with the result with background uncertainty. In this example $SES = 0.5$ and $d = 2$. The background prediction goes from 0.1 to 2.5. See Fig. 12 for the result. Some conclusion can be drawn in this paragraph. Less background gives larger test statistics and central value of BR. The CL_s curve with less background is always on the right side of one with higher background. In addition less background usually gives smaller 68% confidence interval like the way implemented in this note. If the 68% interval is chosen as $CL_s \in [0.32, 1]$ it will gives larger range in BR.

Background uncertainty Do another imaginary integral for background uncertainty. Set $SES = 0.5$, $b = 1.3 \pm 0.4$ and no error for SES which will give a plot shown in Fig. 13. The curve with background uncertainty is always on the right side of the one without background error, however it does not make sure the one with background error will give a larger confidence interval. For example for this case if choosing $CL_s \in [0.2, 0.4]$ a smaller interval is got.

13.1.6 An example for two cells

Two cells situation is simplest case to study junk method. Some problems with junk method will appear here. They will give a hint on how to understand the final pnn result.

Increase of candidates in one of two cells This test is very simple. Cell 1 and 2 both have $SES = 0.5$ and $b = 0.2$ whose error are all 0. Cell 2 has 0 candidate. Cell 2 has 0 to 5 candidates. See Fig. 14 for the result. With the increase of candidates number the central value and 68% interval position both increase simultaneously.

CL_s **curve may not be continuous** CL_s curve is supposed to be continuous. So the confidence interval can be figured out through it. However in junk method this requirement is not perfectly met. There will be some ambiguity when trying to get the final result. When the cell numbers increase or the uncertainty is considered in the calculation this behavior will be not very obvious, but it still exist.

When evaluating $P(s+b)$ and $P(b)$ (see Equ. 62) the test statistic of each candidates combination X_α is compared with the observed one X_{obs}. With the increase of s (for a

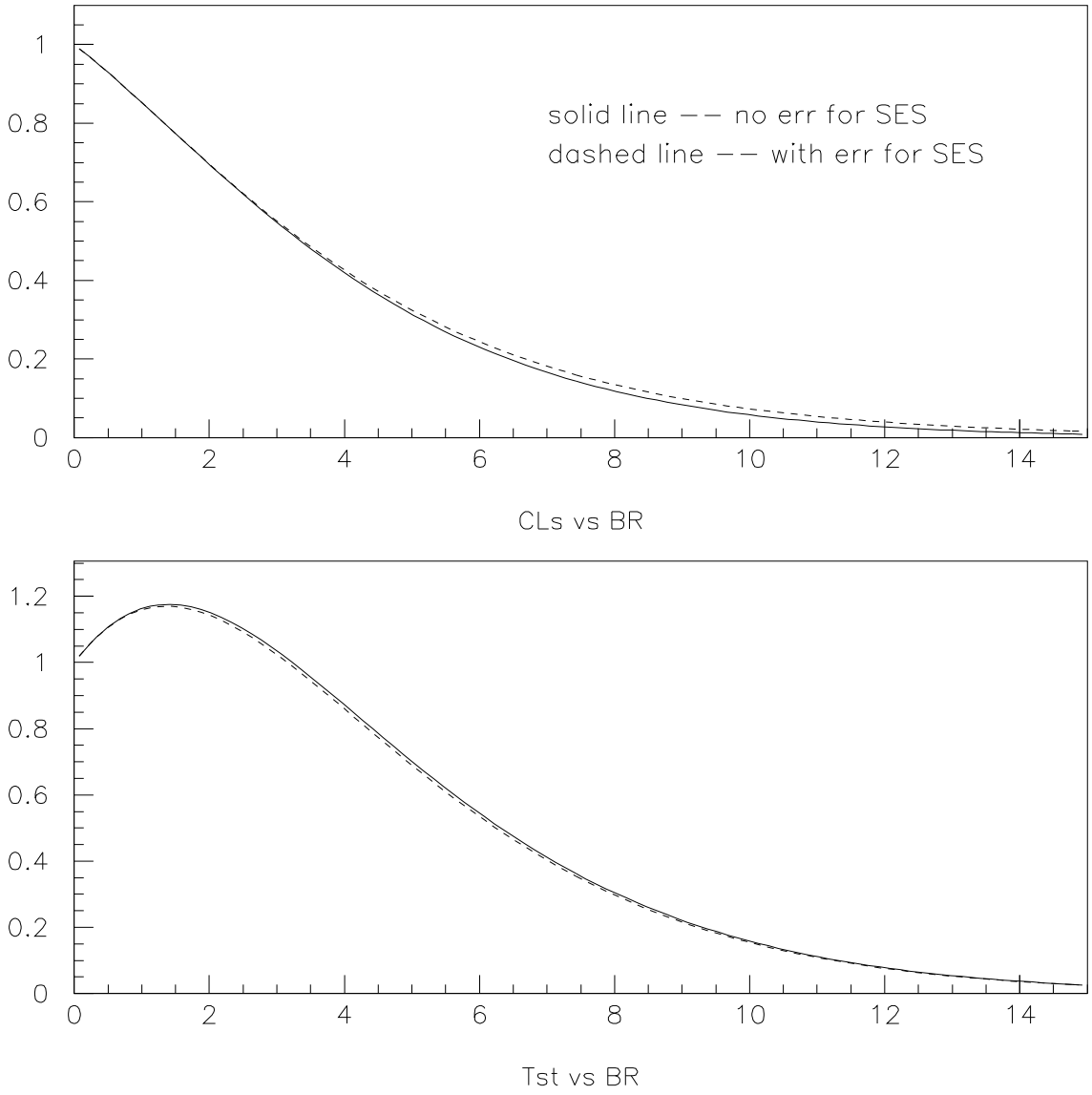

Figure 11: One cell with SES uncertainty. The plot on the top is for CL_s, the one on the bottom is for test statistics.

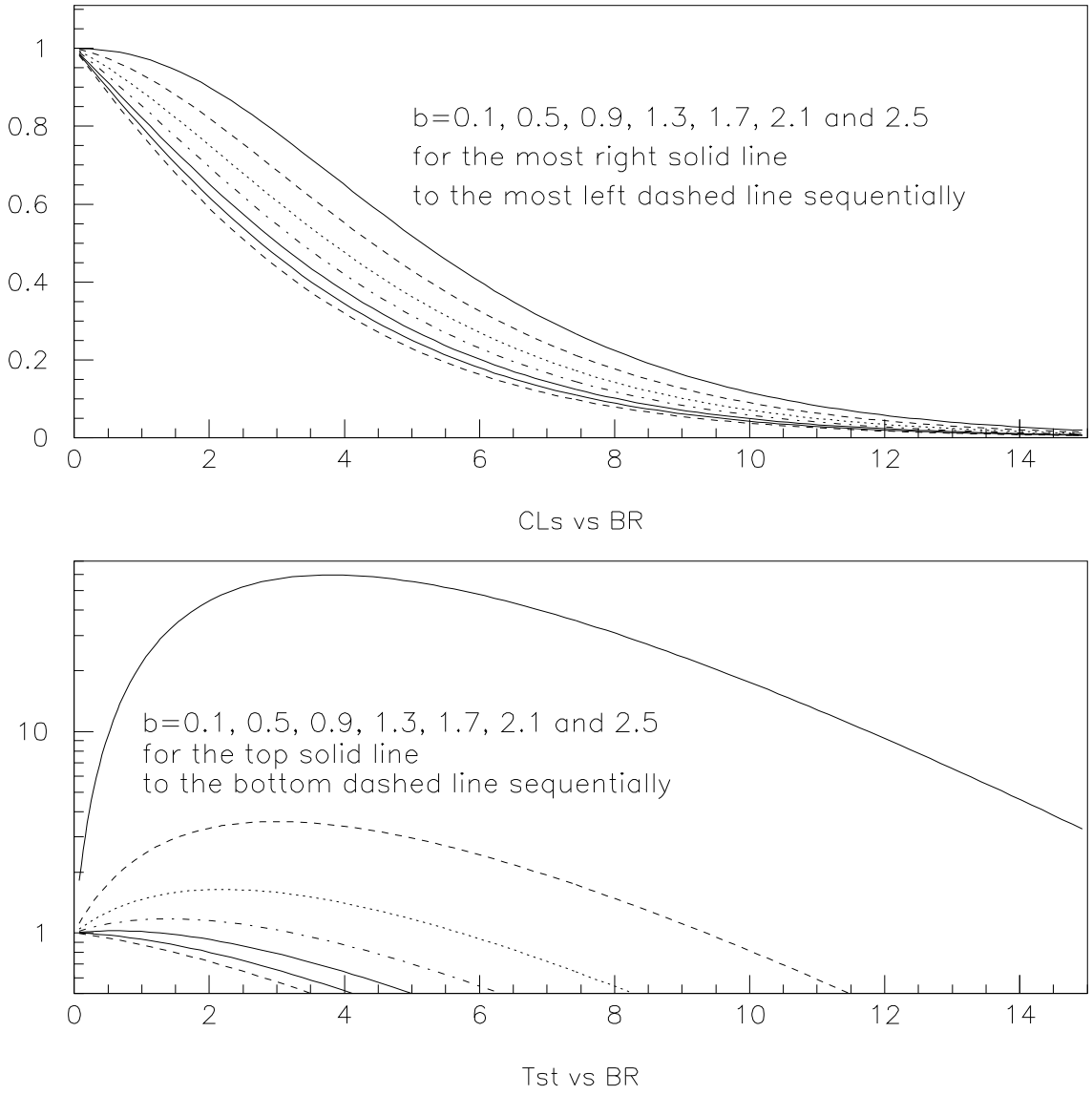

Figure 12: One cell with increasing background. The plot on the top is for CL_s, the one on the bottom is for test statistics.

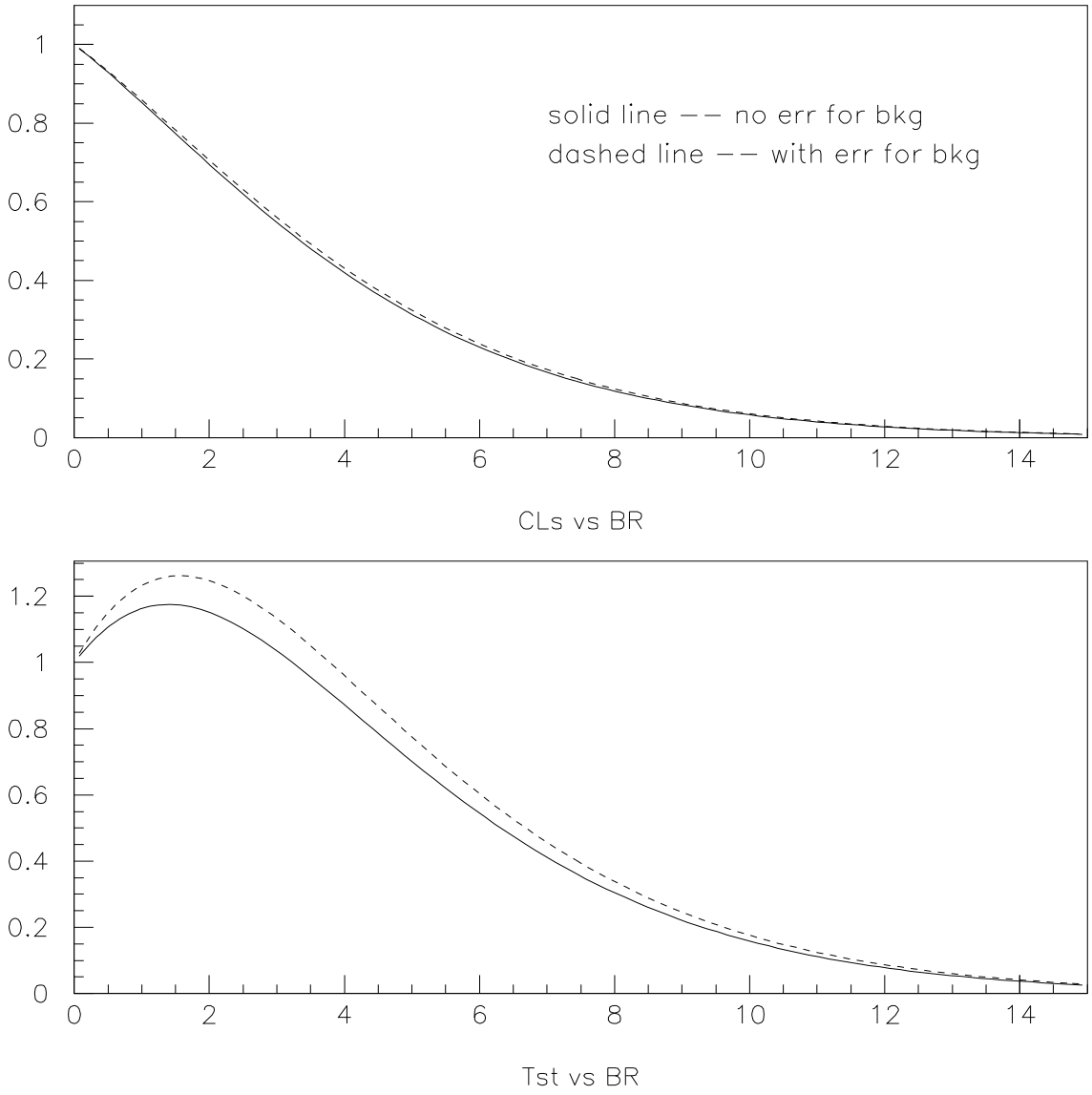

Figure 13: One cell with background error. The plot on the top is for CL_s, the one on the bottom is for test statistics.

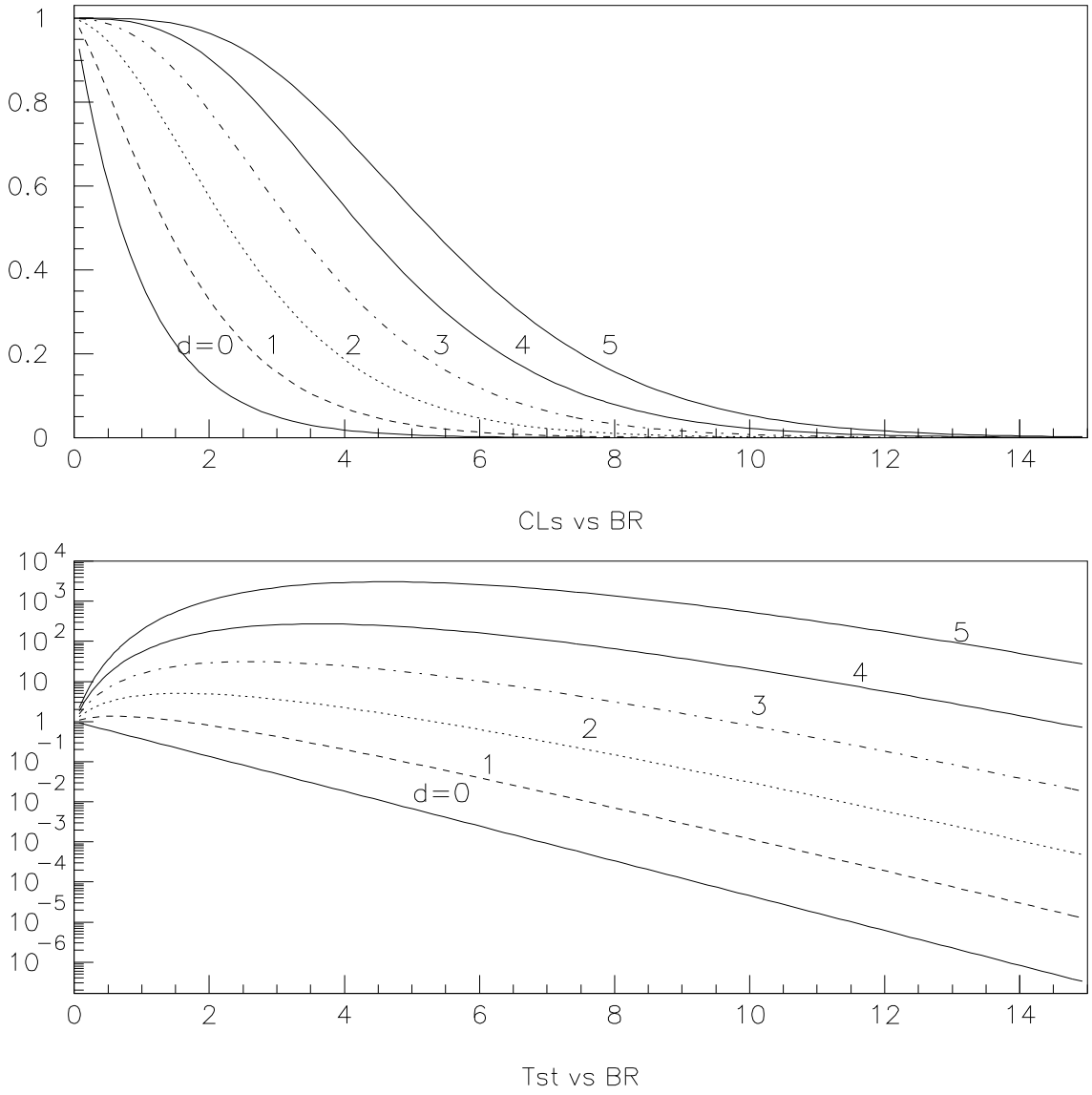

Figure 14: Increase of candidates in one of two cells. The plot on the top is for CL_s, the one on the bottom is for test statistics. Candidates number is labeled on each curve.

fixed SES with the increase of BR) the X_α might cross X_{obs} at some point. So the sum of $P(s+b)$ or $P(b)$ will suddenly include or drop the contribution from one combination. Now the choice of X is likelihood ratio which probably is not the best option. However choosing a new X may not the essential solution of junk method.

Here an example is given to get some feeling about this issue. Assume $SES_1 = 0.2$, $b_1 = 0.2$, $d_1 = 2$, $SES_1 = 0.5$, $b_1 = 0.2$ and $d_2 = 0$. Result is shown in Fig. 15. The CL_s curve for (2,0) is not continuous. The reason is that $X(2,0)$ and $X(0,1)$ intersect. (In this paragraph the two integers in parentheses is the candidates number in the 1st and 2nd cell respectively.)

Increase of SES Here a simple example is given on two cells case with different SES. The specific number using in this test are: $SES_1 = 0.2, 0.3, 0.4, 0.5, 0.6, 0.7, 0.8$, $b_1 = 0.2$, $d_1 = 2$, $SES_2 = 0.5$, $b_2 = 0.2$ and $d_2 = 0$. See Fig. 16 for the CL_s and test statistics curves of them. An obvious defect is when BR is around 2 all the CL_s curves are on the left side of the one with $SES = 0.5$. No matter SES increase or decrease they all lead to smaller CL_s. And they don't show any possible regular pattern. This is against the intuition. The surface reason is the choice of test statistic. The way of calculating P_{s+b} or CL_s is also questionable. Following this property is that the behavior of CL_s curves with uncertainties will be out of control and show some 'random' character. When the number of observed candidates is small this is not serious problem. The test statistic still works well like one cell case.

SES **uncertainty** In this example every setting is the same with previous test, ie. $b_1 = 0.2$, $d_1 = 2$, $SES_2 = 0.5$, $b_2 = 0.2$ and $d_2 = 0$, except that $SES_1 = 0.5 \pm 0.1$. The CL_s and test statistic curves is shown in Fig. 17. Obviously the one with uncertainty gives smaller 68% interval.

Different background and background error The same work is done with background numbers. There is no transparent conclusion. b appears in numerator and denominator. CL_s and X are both complex functions of that.

Other comment Another interesting plot is shown in [10], Fig. 88. The so-called "pdf" is not consistent with X_{obs} as a function of branching ratio.

13.2 BR measurement

The branching fraction of pnn rare decay is calculated with junk method. The error of branching fraction is dominated by statistical uncertainty of candidates number. When taking the error of background and sensitivity into account the central value of BR will change only one or two percent and it has minor impact on 68% interval.

Background and sensitivity numbers are collected from previous E787 and E949 publications. When they are not interpreted there previous analysis notes are scanned to find the number. Some help are provided by previous E949 pnn1 analysis junk code for the detailed information of the 98's 486 and 2002's 3781 cells.

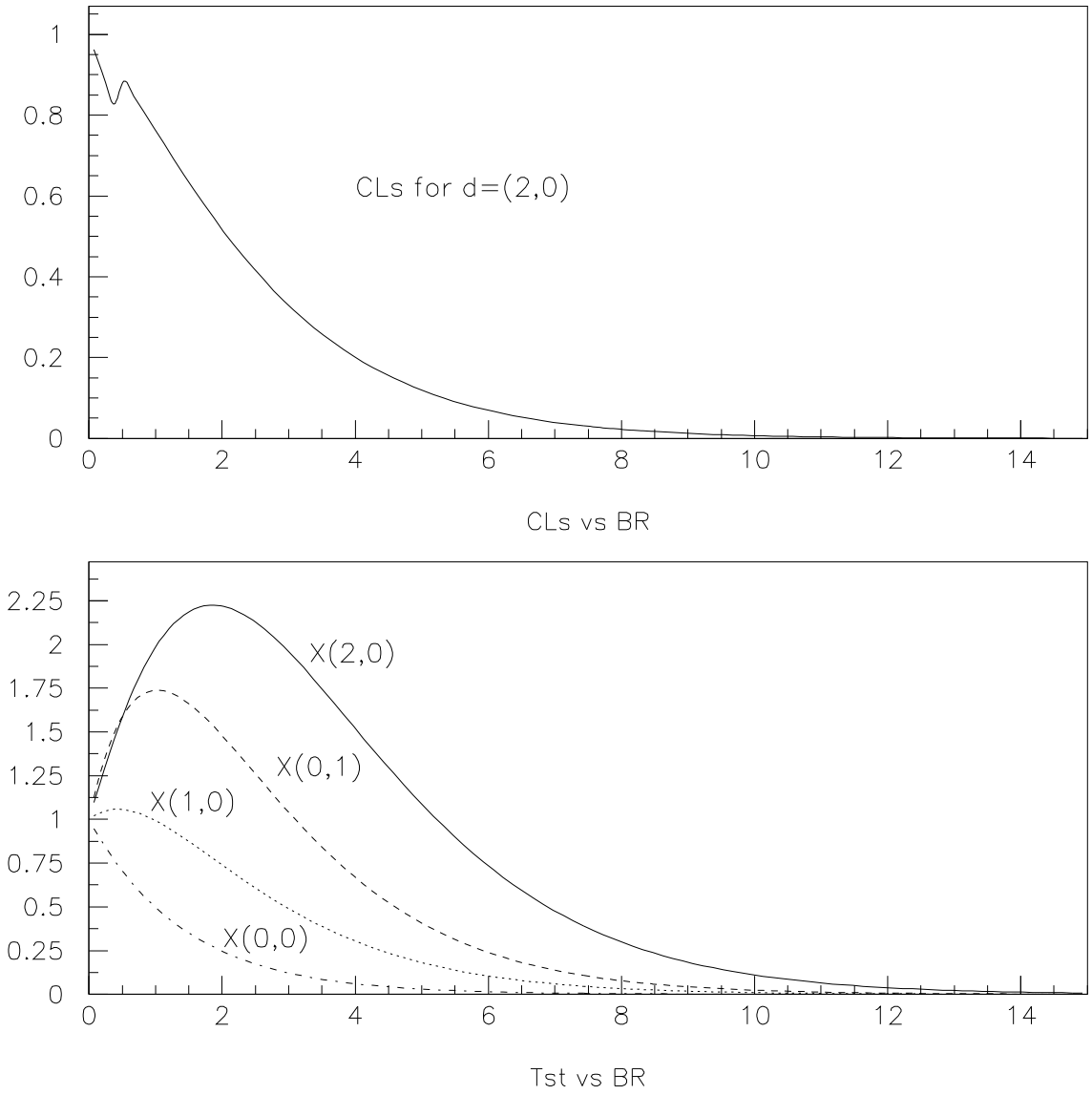

Figure 15: CL_s curve may not be continuous. The plot on the top is for CL_s, the one on the bottom is for test statistics. See text for detailed explanation.

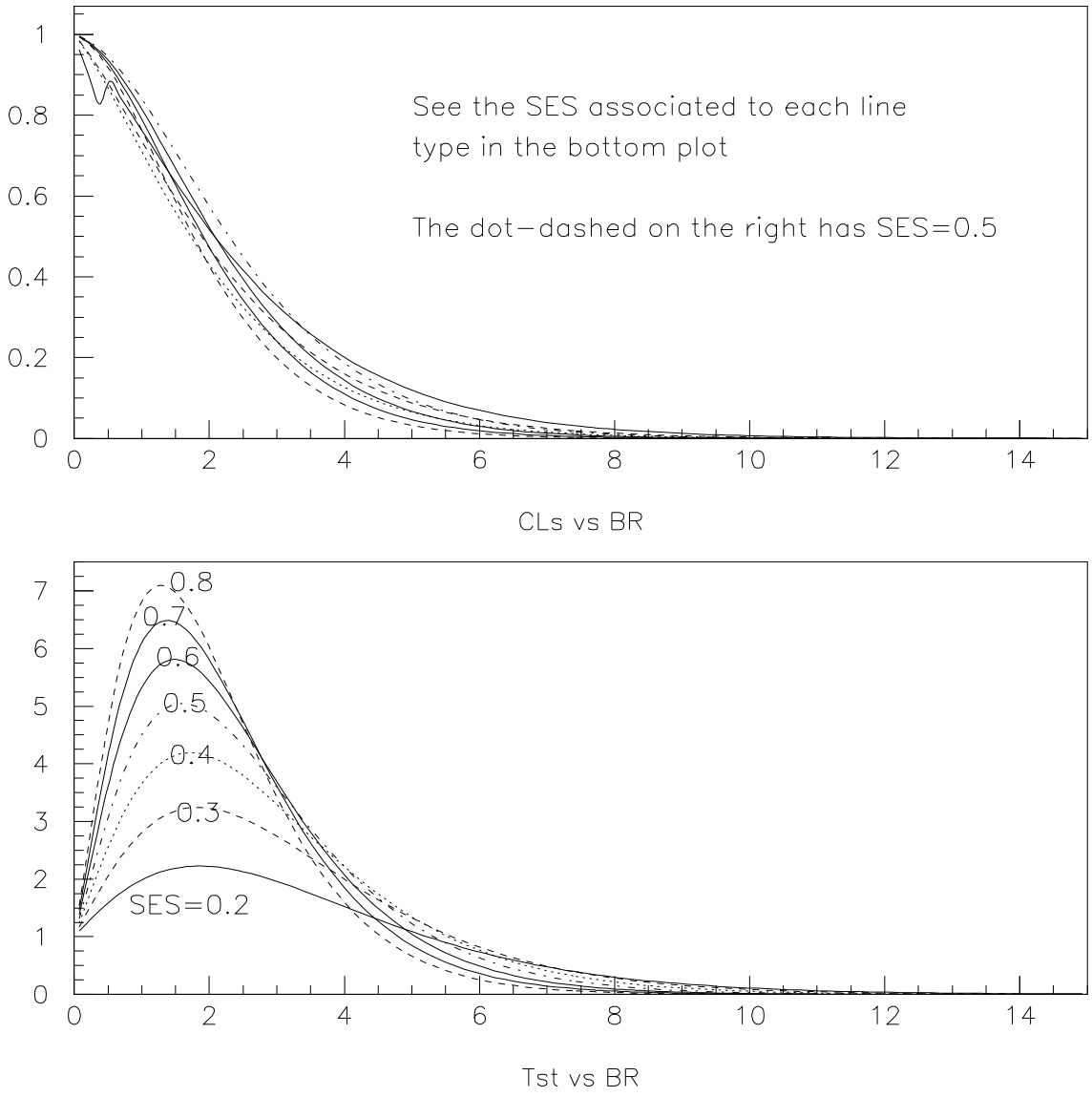

Figure 16: Two cells with different SES. The plot on the top is for CL_s, the one on the bottom is for test statistics. See text for detailed explanation.

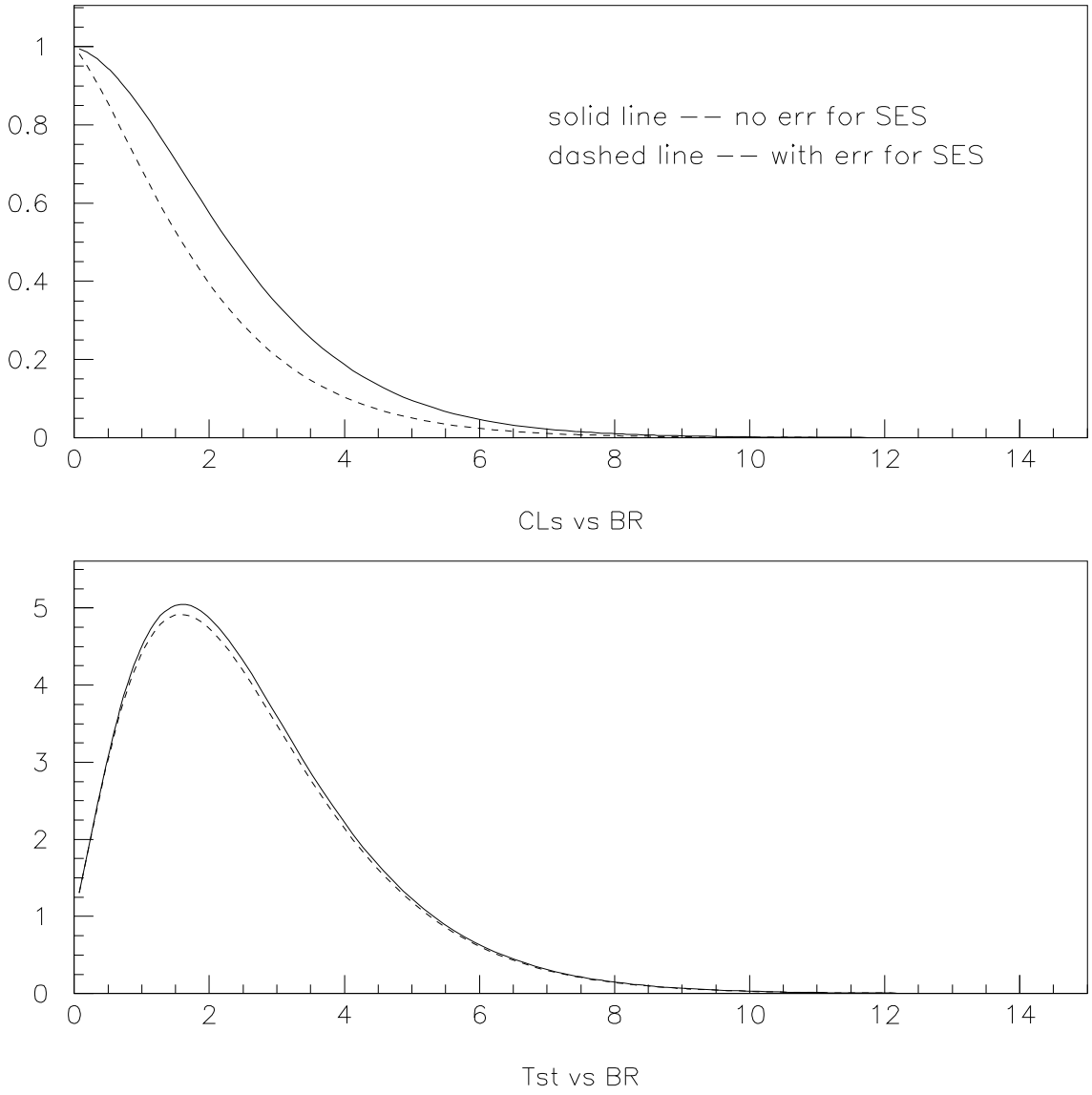

Figure 17: Two cells with SES error. The plot on the top is for CL_s, the one on the bottom is for test statistics.

In this analysis 7 cells are defined for all pnn1 result like presented in 2002 pnn1 paper. Two cells are for 95 97 data. 486+3781 cells are sorted according to their Acc/Bkg and they are grouped into five cells. Two are for candidates cells and three empty cells. One empty cell is the sum of all the empty cells with Acc/Bkg less than candidate cell 1, one is with Acc/Bkg greater than candidate cell 2 while another one is in between. One cell is defined for each of 96 and 97 pnn2 data. So there are totally 9 cells for previous analysis. 9 cells for this E949 pnn2 study. They add up to 18 cells in this estimation.

Background uncertainties is considered in this calculation as independent gaussian fluctuation. Correlated 10% uncertainty is assigned to every year's sensitivity result.

13.2.1 1/3 sample result

See Tab. 38 for the result. In addition Fig. 18 presents the CL_s and test statistics curves for the case with errors.

	BR (with err)	BR (without err)
pnn1	$1.46^{+1.36}_{-0.87}$	$1.47^{+1.34}_{-0.89}$
pnn1+E787,pnn2	$1.41^{+1.33}_{-0.82}$	$1.42^{+1.34}_{-0.83}$
all, 9 empty cells	$1.21^{+1.31}_{-0.63}$	$1.22^{+1.32}_{-0.63}$
one Can in cell #1 (worst)	$1.29^{+1.29}_{-0.71}$	$1.29^{+1.30}_{-0.70}$
one Can in cell #2 (best)	$1.50^{+1.26}_{-0.85}$	$1.50^{+1.26}_{-0.84}$
one Can in cell #3	$1.43^{+1.27}_{-0.82}$	$1.43^{+1.28}_{-0.81}$
one Can in cell #4	$1.32^{+1.29}_{-0.73}$	$1.31^{+1.30}_{-0.72}$
one Can in cell #5	$1.31^{+1.29}_{-0.72}$	$1.30^{+1.30}_{-0.72}$
one Can in cell #6	$1.46^{+1.26}_{-0.83}$	$1.46^{+1.27}_{-0.82}$
one Can in cell #7	$1.41^{+1.27}_{-0.81}$	$1.40^{+1.28}_{-0.80}$
one Can in cell #8	$1.31^{+1.29}_{-0.72}$	$1.30^{+1.30}_{-0.72}$
one Can in cell #9	$1.30^{+1.29}_{-0.72}$	$1.30^{+1.30}_{-0.71}$

Table 38: BR measurement of 1/3 sample with or without uncertainties.

13.2.2 2/3 sample result

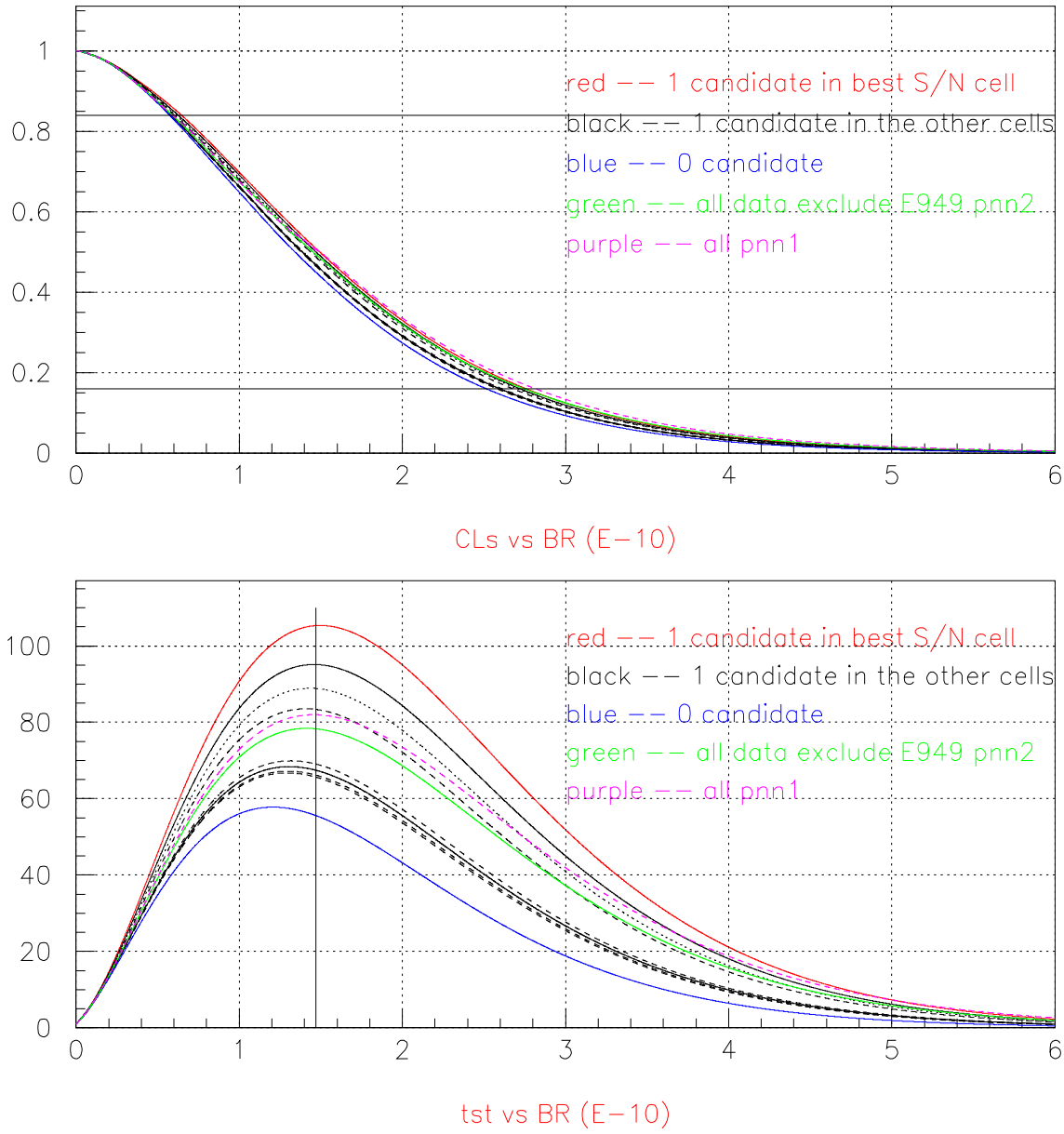

Figure 18: CL_s and test statistic curves for BR measurement in 1/3 sample. The two horizontal lines in the upper plot indicates the 68% coverage and the vertical line in the bottom plot indicates the published central value in 2002 pnn1 paper.

References

[1] J.Ives et. al. "PNN2 1/3 Analysis", "Analysis of the 1/3 E949 pnn1 data", E949 Technical Note **K-073**.

[2] M. Diwan, et. al. "PNN2 1/3 Analysis", "PNN2 2/3 Analysis", E787 Technical Notes **tn385**, **tn386**, 2001.

[3] I. Christidi, "Search for the rare decay $K^+ \to \pi^+\nu\bar{\nu}$ with $p_{\pi^+} < 199$ MeV/c", Ph.D. thesis, 2006

[4] Vivek Jain, "Simulation of elastic scatters of pi+ in the target from Kp2 decays" E787 Technical note 375, 3 November 1999.

[5] B. Lewis, "PNN2 1/3 Beam Background", E949 Technical Note **K-061**, 2006. Unpublished.

[6] S. Chen *et al.*, "2002 pnn1 Data Analysis", E949, note K-034 (2003).

[7] Bipul Bhuyan, Ph. D thesis (2003).

[8] B. Lewis, "Addition to Bad Runs List", E949 Technical Note **K-060**, 2006. Unpublished.

[9] Thomas Junk, "Confidence level computation for combining searches with small statistics", NIM, A434 (1999) 435-443.

[10] S. Chen *et al.*, "Further 2002 pnn1 Data Analysis", E949, note K-038 (2004).